44-1319

EA-77-A-01-6010-9
Distribution Category UC-90g

DEVELOPMENT, TESTING AND EVALUATION OF MHD-MATERIALS

Quarterly Report

for the period July - September 1977

H. P. R. Frederikse, T. Negas and S. J. Schneider

Inorganic Materials Division
Institute for Materials Research
National Bureau of Standards
Washington, D. C. 20234

Date Published: September 30, 1977

PREPARED FOR THE UNITED STATES
ENERGY RESEARCH AND DEVELOPMENT ADMINISTRATION
Under Contract No. E(49-1)-3800

TABLE OF CONTENTS

ABSTRACT

During this quarter preparations went forward for the testing of an electrode/insulator assembly in the U-02 facility under auspices of the US-USSR cooperative program on MHD power generation (Phase III). Samples of various electrode materials to be used in this test were received from the Westinghouse Research Laboratories and from other organizations for determination of their electrical conductivity.

Some 60 materials were analyzed by X-ray diffraction with regard to crystallinity and phase composition.

Further progress was made on the seed-slag interaction problem by mapping major sections of the phase diagram for the system K_2O-CaO-Al_2O_3-SiO_2.

A set of 11 cathodes and anodes was delivered to AVCO and tested in their Mark VI MHD channel under slagging conditions on September 14, 1977.

Characterization of six electrodes tested in the MIT rig in May of this year was completed. It appeared that the HfO_2- and ZrO_2-based caps had separated completely from the underlying spinel on the cathode side.

Samples of chrome-magnesia, tested for 30 hrs. in a seed environment, were received from the Fluidyne Engineering Corporation, and examined by means of X-ray diffraction and Scanning Electron Microscopy.

A list was compiled of references to property data for some 20 stainless steels and alloys which show promise for use in downstream components of MHD systems.

Objectives and Scope of Work

The overall objective of this program is to obtain chemical and physical definition of high temperature materials which have shown promise for use in coal-fired open-cycle MHD power systems. Major problem areas in which investigations will be concentrated are:

1. Characterization of coal slag and its effects on system components and performance at prototype temperatures.

2. Development of electrode materials which provide adequate performance over extended periods of time.

3. Insulating materials which limit thermal losses and are resistant to prolonged thermal and erosion effects.

4. Preheater materials which can withstand the operating modes of separately and directly fired operation.

5. Seed recovery methods from slag which are technically and economically feasible.

6. Phase equilibria and diffusion rates of seed in slag and the corrosive action of combination on system components and materials.

7. Durability of prototype MHD sub-systems.

The program is designed to contribute to the solution of these problems by providing much needed data on candidate materials and by evaluating test samples and structures that have been subjected to real or simulated MHD conditions. The activities are grouped under six tasks:

G. Program Management Coordination (Assisting ERDA in coordination, planning and review of the various MHD-Materials Development Programs).

H. U-02 Materials Testing and Characterization (Coordination of U-02 Test Activities, Phase I). (Terminated June 30, 1976).

I. Operational Design Properties (viscosity, electrical conductivity, vaporization).

J. Corrosion by Seed and Slag (phase equilibria, diffusion).

K. Materials Testing and Characterization (test coordination, pre- and post-test analysis).

L. Assessment of Steam Plant Components (corrosion resistance of metals and alloys).

Summary of Accomplishments (July-Sept. 1977)
(Completed Milestones - see Work Statement for FY 1977)

The results obtained during the 4th Quarter are presented in terms of the projected milestones of the NBS-ERDA Contract.

1c. Reviewed together with participating groups the status of preparations made by the Westinghouse staff for the Phase III, U-02 materials test planned for early 1978.

2a. Participated in a number of program coordination meetings and technical conferences including the ERDA Workshop on Materials (Germantown, MD, 7/13/77).

b. S. J. Schneider and H. P. R. Frederikse attended as observers a 12-hour test of electrode/insulator assemblies in the Mark VI at the AVCO Everett Research Laboratories.

5b. Determined the effects of CaO and MgO additions and deletions on the viscosity of coal slag.

19b. Measured the electrical conductivity of a number of electrode materials (prepared by Westinghouse, G.E. and ANL) for the Phase III-U-02 test.

39c. Analyzed by means of X-ray diffraction and Scanning Electron Microscopy several electrode and preheater materials that were tested in various test rigs (MIT, Fluidyne).

43. Updated a list of references to properties of promising wrought alloys (stainless steels, Ni- and Co-based alloys), including cost.

Talks and Publications

MHD-Materials
S. J. Schneider, T. Negas and H. P. R. Frederikse
Proc. of the Colloquium on Refractory Oxides for High Temperature Energy Sources, Odeillo, France, July 1977.

Spinels as MHD-Generator Wall Materials
W. R. Hosler
American Ceramic Society (Electronics Division)
Montreal, Quebec, Canada, September 1977.

Preparation and Properties of CeO_2-HfO_2 Electrodes for MHD Applications
J. W. Hafstrom and J. T. Durek (ANL), J. L. Bates (Battelle NW), and T. Negas (NBS)
American Ceramic Society (Basic Science and Nuclear Division)
Hyannis, Mass., September 1977.

TASK G. PROGRAM MANAGEMENT AND COORDINATION (S. J. Schneider)

1. Program Review and Consultation Activities

S. J. Schneider participated in assorted ERDA-arranged or sanctioned program review/coordination meetings, briefings and technical conferences. These included:

1. Alcoa Laboratories, Pittsburgh, July 18-19, 1977 (Lecture plus consultation on MHD materials applications).

2. Colloquium on Refractories for Energy, Odeillo, France, June 30 - July 3, 1977. (Invited lecture on MHD Materials.)

3. Materials Ad Hoc Working Group Meeting, Westinghouse, Pittsburgh, July 14, 1977 (U-02 Phase III).

4. ERDA Workshop on Materials, Germantown, July 13, 1977. (Organized by Division of Physical Research, ERDA.)

In addition, NBS hosted a number of visitors from MHD contractors (and others interested in MHD) to consult on a variety of specific topics. During this quarter, visitors included representatives from Stanford, MIT, Montana TECH, MSU, CEGB (England), and Petten Establishment (The Netherlands). The conclusions and recommendations resulting from these meetings and other ERDA-assigned activities are reflected in reports to ERDA, through direct consultation with ERDA staff or through documents published elsewhere.

NBS receives on a regular basis, MHD technical reports and proposals for review. During this period NBS provided 1 such evaluation.

Part of the NBS experimental program involves characterization of materials component elements tested in various MHD test rigs and facilities throughout the United States (and USSR). In order to expedite the dessimination of this information, NBS has instituted a separate reporting system in addition to the regular Quarterly submissions. The system consists of the following elements: 1. Telephone report to submittor after initial examination, 2. Follow-up letter report, and 3. Detailed report (if warranted) to submittor and ERDA. The detailed report will be distributed to general contractors on an as-needed-basis as determined by ERDA; however, highlights of the detailed report will be abstracted and published in the NBS Quarterly reports. In addition, general overall summary reports will be compiled from time to time and published in appropriate journals and special editions.

Inquiries regarding the status of any particular characterization or requests for additional assistance should be directed to:

A. Perloff, 301-921-2900

alternates:
T. Negas, 301-921-2843
W. Hosler, 301-921-2940

During this period, a detailed technical review of the Phase III, U-02 activity was held at the Westinghouse Research Laboratory. The overall effort is being managed by Westinghouse; other participating groups include NBS, Battelle-NW, ANL and GE. The minutes and recommendations resulting from this meeting are on file at ERDA. As a follow-up, NBS requested a complete review of the anticipated electrode loading scheme for both the proof tests and the actual U-02 experiment; this has been done (by Westinghouse) and the current thinking will be incorporated in appropriate work and test plans.

In addition to the above, the final draft of the Joint US-USSR chapter on materials (Status Report) has been proof-read and final corrections inserted. Publication is expected during the next quarter.

Task I. OPERATIONAL DESIGN PROPERTIES

1. Viscosity of Coal Slags (W. Capps and D. A. Kauffman, Inorganic Glass Section)

Introduction

As the number of laboratories investigating various aspects of coal-fired, open-cycle MHD has increased so has the tendency to experiment with two specific sources of coal. These are Montana Rosebud Seam Coal, typical of western sub-bituminous coals and Illinois #6, typical of mid-western sub-bituminous coals.

The NBS program, therefore, has concentrated recently on these two types of coal for its slag experiments.

Slag Preparation and Viscosity Measurements

A series of synthetic slags was prepared in order to assess the contribution of each oxide component to the viscosity of the slag. A composition for the starting point or the "base" composition was chosen that is between the Rosebud and the Illinois #6 slags. Each of these types varies over a wide range; a large number of ash analyses from each coal type was averaged. The NBS "base" composition was the average of these two averages. This means that the SiO_2 content of the base was averaged, the Al_2O_3 content was averaged, etc.

To this base composition SiO_2 was added in 5% increments or removed in 5% increments keeping the other oxides in constant proportion. Next Al_2O_3, Fe_2O_3, CaO and MgO were altered incrementally. The report for the period ending on December 31, 1976, showed the results of the SiO_2, Al_2O_3 and Fe_2O_3 changes.

This report gives the results of the changes of CaO and MgO on viscosity.

Figure 1 shows the effect of the CaO and Figure 2 the effect of the MgO variations.

Table 1 shows the compositions of these melts.

Two observations can be made at this time. CaO has a strong fluxing action, reducing the viscosity markedly but not quite as much as the corresponding wt % additions of Fe_2O_3. MgO is the strongest agent in reducing viscosity on a wt % basis but is usually present in smaller amounts than the other oxides.

The data is being analyzed in order to select that mathematical model which will best describe the viscosity of slags from these two coals as functions of ash composition and melt temperature.

Future Plans

A number of methods will be compared to select the best method for estimation of coal slag viscosity.

Table 1

Coal Slag Compositions (wt %)

NBS Melt No.	SiO_2	Al_2O_3	Fe_2O_3	CaO	MgO	
K-884	47.77	21.76	16.58	10.57	3.32	Base
K-960	45.10	20.54	15.65	15.57	3.13	+ 5% CaO
K-965	42.43	19.33	14.73	20.57	2.95	+10% CaO
K-969	50.44	22.97	17.51	5.57	3.50	- 5% CaO
K-971	53.42	24.33	18.54	--	3.71	-10.57% CaO
K-973	39.76	18.11	13.80	25.57	2.76	+15% CaO
K-976	45.30	20.63	15.72	10.02	8.32	+ 5% MgO
K-980	42.82	19.51	14.87	9.48	13.32	+10% MgO
K-985	49.41	22.51	17.15	10.93	--	- 3.32% MgO

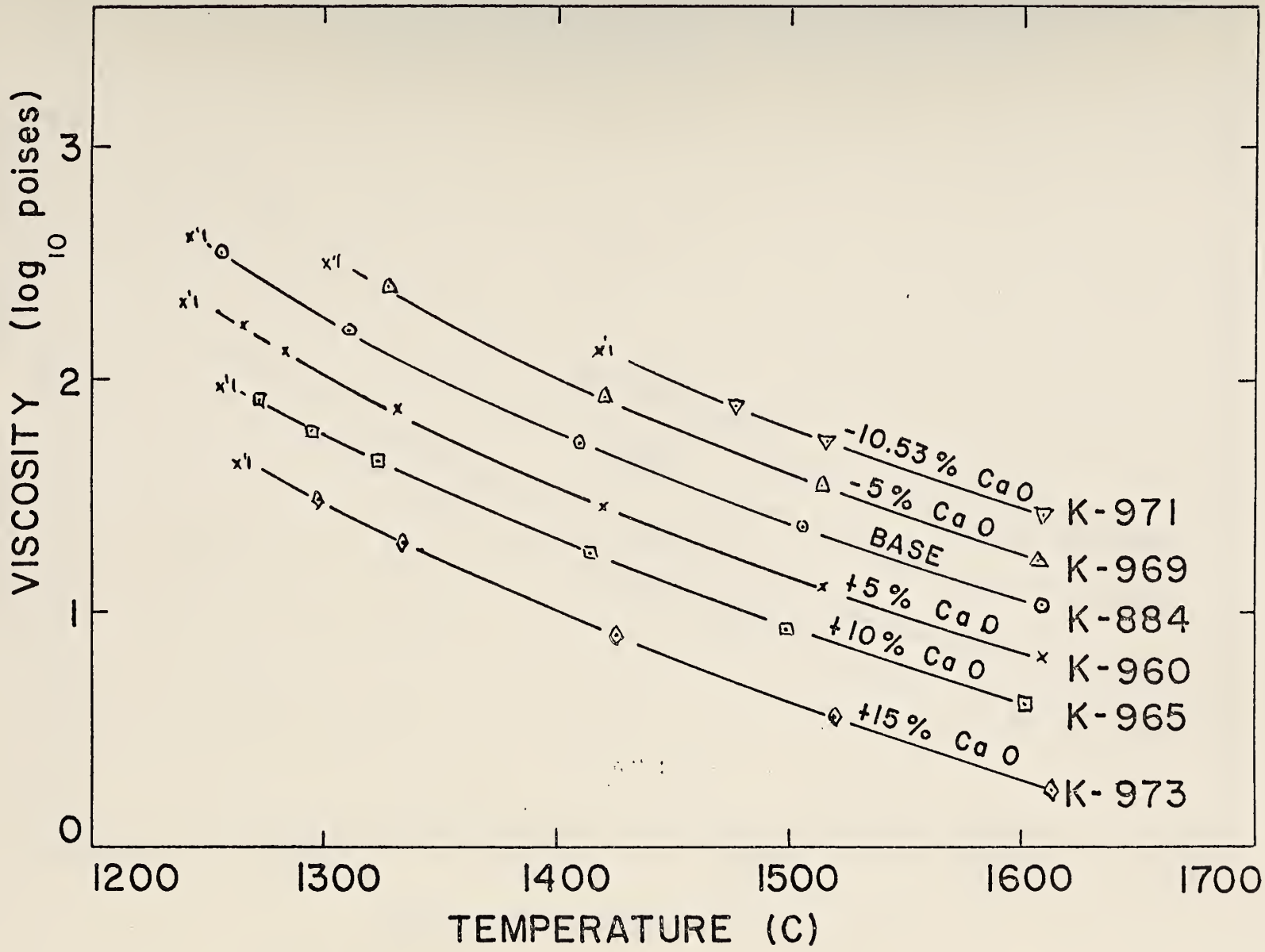

EFFECT OF CaO ADDITIONS

Fig. 1.

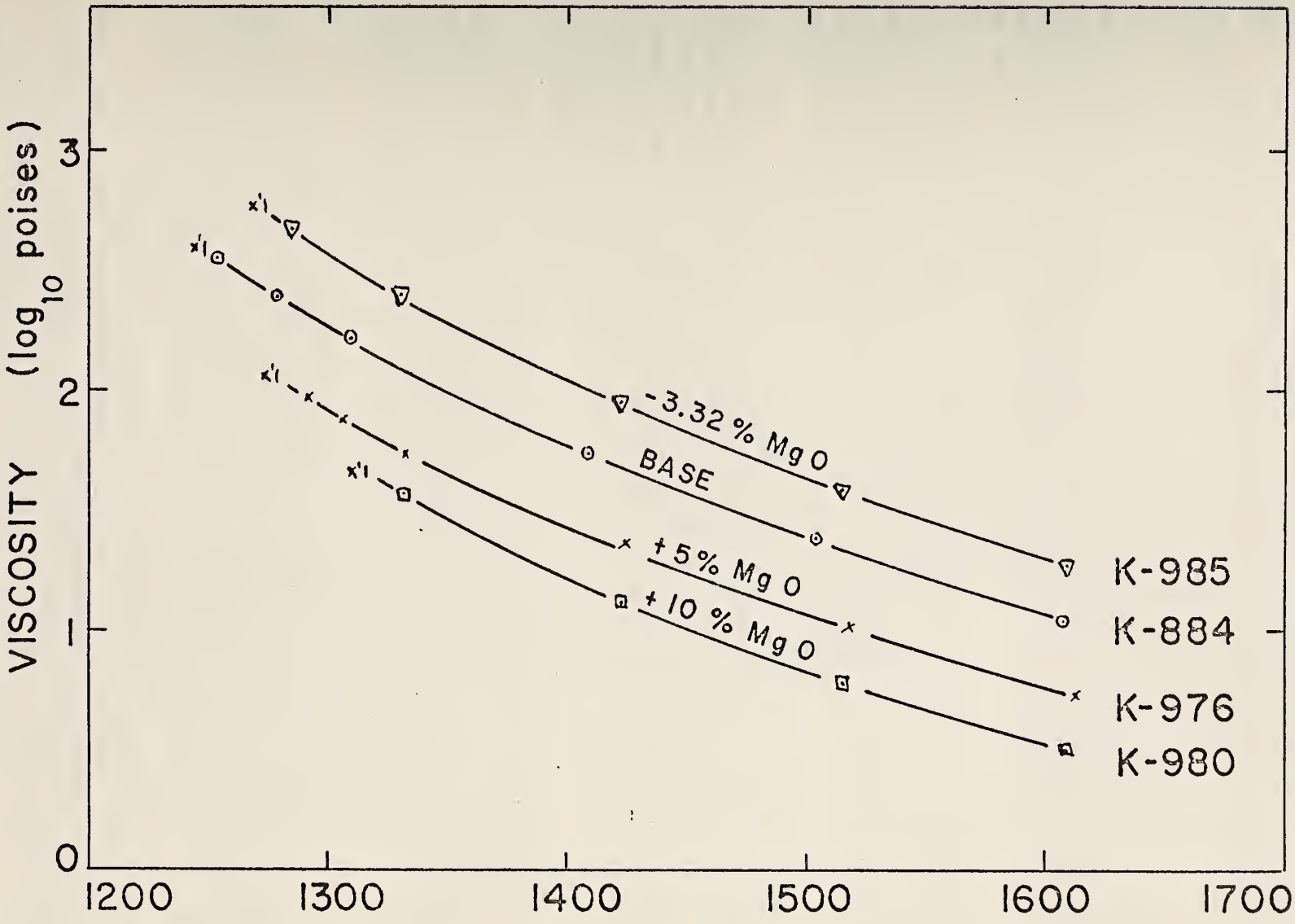

EFFECT OF Mg O ADDITIONS

Fig. 2.

2. Electrical Conductivity (W. R. Hosler and A. J. Armstrong)

$K_2O \cdot 7[Fe_{1.95}Ti_{.05}O_3]$. Several samples of potassium ferrites were made but T. Negas of NBS. During the conductivity measurements, drifting of voltages and currents was a problem and an attempt to reproduce the data obtained was not successful. Work is underway to construct a test cell in which we can measure the conductivity of this and other materials under different pressures of potassium.

$SrZrO_3$. A sample of $SrZrO_3$ designated SZ-UMO101 was received from Westinghouse Research and Development Laboratory, Pittsburgh, PA. This was a high purity sintered piece mentioned in our previous Quarterly Report (April-June 1977). The electrical conductivity of this material (see Fig. 3) appears to be higher than desired at elevated temperatures for it to be used as an effective insulator for MHD electrodes.

An attempt was made to lower the electrical conductivity of $SrZrO_3$ by substituting small amounts of La for Sr in a 2 to 3 ratio. A sample of $Sr_{.97}La_{.02}ZrO_3$ was made by H. U. Anderson of A T Research and its electrical conductivity was measured (see Fig. 4). By comparing Figures 3 and 4, it can be seen that the electrical conductivity was indeed lowered but not sufficiently to make the material viable as an MHD insulator.

Four samples have been received from H. U. Anderson of A T Research in which various amounts of La and Cr were substituted into $SrZrO_3$. Two of these samples have been measured (see Figs. 5 and 6) and the effect of the substitutions ia a slight increase in electrical conductivity at high temperatures with a substantially greater increase in conductivity at lower temperatures. Measurements are in progress on the two remaining samples ($Sr_{.9}La_{.1}Zr_{.9}Cr_{.1}O_3$ and $Sr_{.9}La_{.1}Zr_{.7}Cr_{.3}O_3$) and will be reported in our next Quarterly Report.

85 m/o ZrO_2 - 12 m/o CeO_2 - 3 m/o Y_2O_3. Two samples of composition 85 m/o ZrO_2 - 12 m/o CeO_2 - 3 m/o Y_2O_3 were received from Westinghouse Research and Development Laboratory, Pittsburgh, PA. The sample designated CZ-CEO101 was prepared by sintering and was found to have a lower electrical conductivity (see Fig. 7) than did sample CZ-CEO201 (see Fig. 8) which had been hot-pressed.

$LaCrO_3$(:Mg) + [ZrO_2(12% Y_2O_3)]. Two samples of lanthanum chromite plus yttria stabilized zirconia were received from Westinghouse Research and Development Laboratory, Pittsburgh, PA. The zirconia is interdispersed in the $LaCrO_3$ and is intended to make the material more refractory and wear resistant in an MHD environment and yet to maintain the electrical conductivity to low temperatures where attachment to a metal lead-out is simplified.

Figure 9 shows the measurement on this material with 30% yttria stabilized ZrO_2 added. The electrical conductivity is reduced by about a factor of four from that of $La_{.95}Mg_{.05}CrO_3$ over the temperature range measured. The data for $La_{.95}Mg_{.05}CrO_3$ is shown in Figure 8 of Quarterly Report - July-Sept., 1976. The electrical conductivity of this material will be measured down to room temperature at a later date.

Figure 10 shows the electrical conductivity of $LaCrO_3$ containing 40 w/o of yttria stabilized ZrO_2 down to about 550 °C. The data down to near room temperature is shown in Figure 11. It is evident that the conductivity is substantially reduced from that of $La_{.95}Mg_{.05}CrO_3$ and any lead-out connection should be made to operate at 300 °C or above for the material.

Layered Electrodes. Two separate samples composed of 3 different layers each but formed into one composite were received from Westinghouse Research and Development Laboratory, Pittsburgh, PA. In each case the top layer was $La_{.95}Mg_{.05}Cr_{.50}Al_{.50}O_3$, the middle layer $La_{.95}Mg_{.05}Cr_{.68}Al_{.32}O_3$ and the lower layer $La_{.95}Mg_{.05}Cr_{.85}Al_{.15}O_3$. One of the composite samples was hot pressed at the Westinghouse Laboratory while the other was prepared by sintering by H. U. Anderson of A T Research. These layers were separated by cutting with a diamond saw for the electrical measurements shown in Figures 12 and 13. In all cases but one, the effect of the Al additions was a reduction in electrical conductivity. The hot-pressed sample, in all cases but one, had a higher electrical conductivity than the sintered sample. At the request of Barry Rossing of Westinghouse the sample of $La_{.95}Mg_{.05}Cr_{.50}Al_{.50}O_3$ (hot-pressed) was heated in air at 1600 °C for 16 hours and at 800 °C for 80 hours to assure complete oxidation. No changes in electrical conductivity was seen after this treatment.

Spinel. A sample of $MgAl_2O_4 + Fe_3O_4$ spinel was received from General Electric. The precise composition is not known. The electrical conductivity of this sample (see Fig. 14) was slightly lower but very similar to MAFF-31 (see Fig. 1 in April - June, 1976 Quarterly Report).

HfO_2(:CeO_2). Three samples of HfO_2 (:CeO_2) and HfO_2(:CeO_2) plus Y_2O_3 were received from Argonne National Laboratory. A sample of composition 82 m/o HfO_2 - 18 m/o CeO_2 (see Fig. 15) was measured electrically with some swelling, deformation, and void formation. When attempts were made to measure the electrical conductivity of a sample of composition 74 m/o HfO_2 - 16.3 m/o CeO_2 - 9.7 m/o Y_2O_3 gross swelling, deformation and void formation occurred.

It is a possibility that these effects were due to the formation of a low melting eutectic when the sample came in contact with the Al_2O_3 conductivity apparatus. Both samples were stuck to the Al_2O_3 but the sample of composition 74 m/o HfO_2 - 16.3 m/o CeO_2 - 9.7 m/o Y_2O_3 was too firmly attached to be removed. Further investigation of this reaction and further attempts to measure the electrical conductivities of these samples are in progress.

Scanning Electron Microscope Examination of Arc-Plasma Sprayed Materials
(A. J. Armstrong)

Seven samples of arc-plasma sprayed materials were received from APS Materials, Inc., Dayton, OH. These samples were prepared during the investigation of optimizing spraying parameters to obtain sprayed materials of highest density single phase compositions in conjunction with the Phase III-US-USSR materials test. Three of the samples were of MAFF-31,

three more were of $LaCrO_3$ + MgO and the last was of S-71 (pure $MgAl_2O_4$). These samples were sectioned and polished for SEM evaluation by the Solid State Physics Section of NBS. Samples were designated as 71107-1, 71107-2, etc. and will be referred to as sample 1, 2, etc.

Samples 1, 2 and 3 were of MAFF-31. The EDX patterns of all three samples were compared and found to be identical indicating chemical uniformity. The EDX patterns were not compared to any standard so they should be considered indicative only. An examination of the physical bodies was done at 100X and 500X. Sample #3 was seen to have the lowest total porosity with sample #1 second, and sample #2 being highest in total porosity. Sample #1 appears to be the most homogeneous from the standpoint of pore size and pore distribution with samples #2 and #3 both showing regions of high density interdispersed with larger pores. In my opinion, sample #1 is the optimum material.

Samples 4, 5 and 6 were of $LaCrO_3$ + MgO. The EDX patterns of all three samples were examined and small amounts of Al were found in samples #5 and #6. The amounts of La, Cr, and Mg appear to be the same in all three samples. A much greater difference can be seen between these samples than was seen between the samples of MAFF-31. Sample #4 has a higher density than sample #6 which has a higher density than sample #5. All three samples appear to be of similar homogeneity. The optimum choice here is the procedure resulting in sample #4.

Sample 7 was of S-71 ($MgAl_2O_4$). Although light and dark areas may be seen on the photomicrograph, an EDX examination of both areas showed no elemental differences between them. The concentration of Mg and Al were seen to be the same for both areas. The physical body is quite dense, despite its mottled appearance, and has a high degree of homogeneity.

Comparing all the samples with each other leads to the conclusion that sample #7 (S-71) has the lowest porosity with samples #4, 5 and 6 ($LaCrO_3$+MgO) a close second, and samples #1, 2 and 3 (MAFF-31) a distant third.

X-ray diffraction results on these seven materials were obtained from C. L. McDaniel of NBS. Samples 1, 2 and 3 were found to be poorly crystalline spinel. Samples 4, 5 and 6 were found to be $LaCrO_3$ of medium to good crystallinity with from 1 to 5% of an unknown phase present. The unknown phase, although unidentified, does not appear to be Al, Al_2O_3 of MgO. Sample 7 was found to be $MgAl_2O_4$ of medium to good crystallinity.

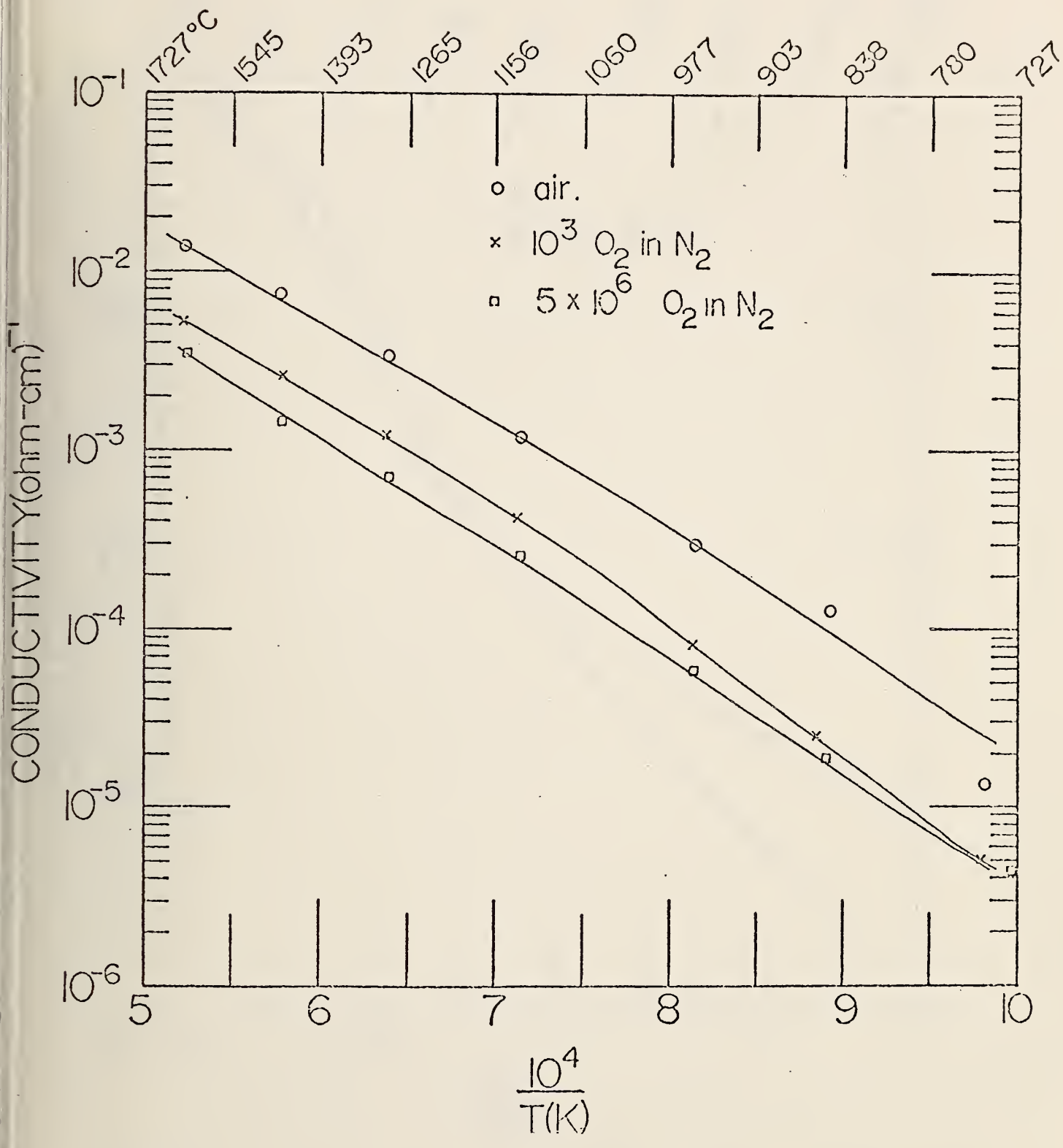

Figure 3. Electrical conductivity of a sample of $SrZrO_3$ from Westinghouse (SZ-UMO101) sintered four hours at 1650 °C in air.

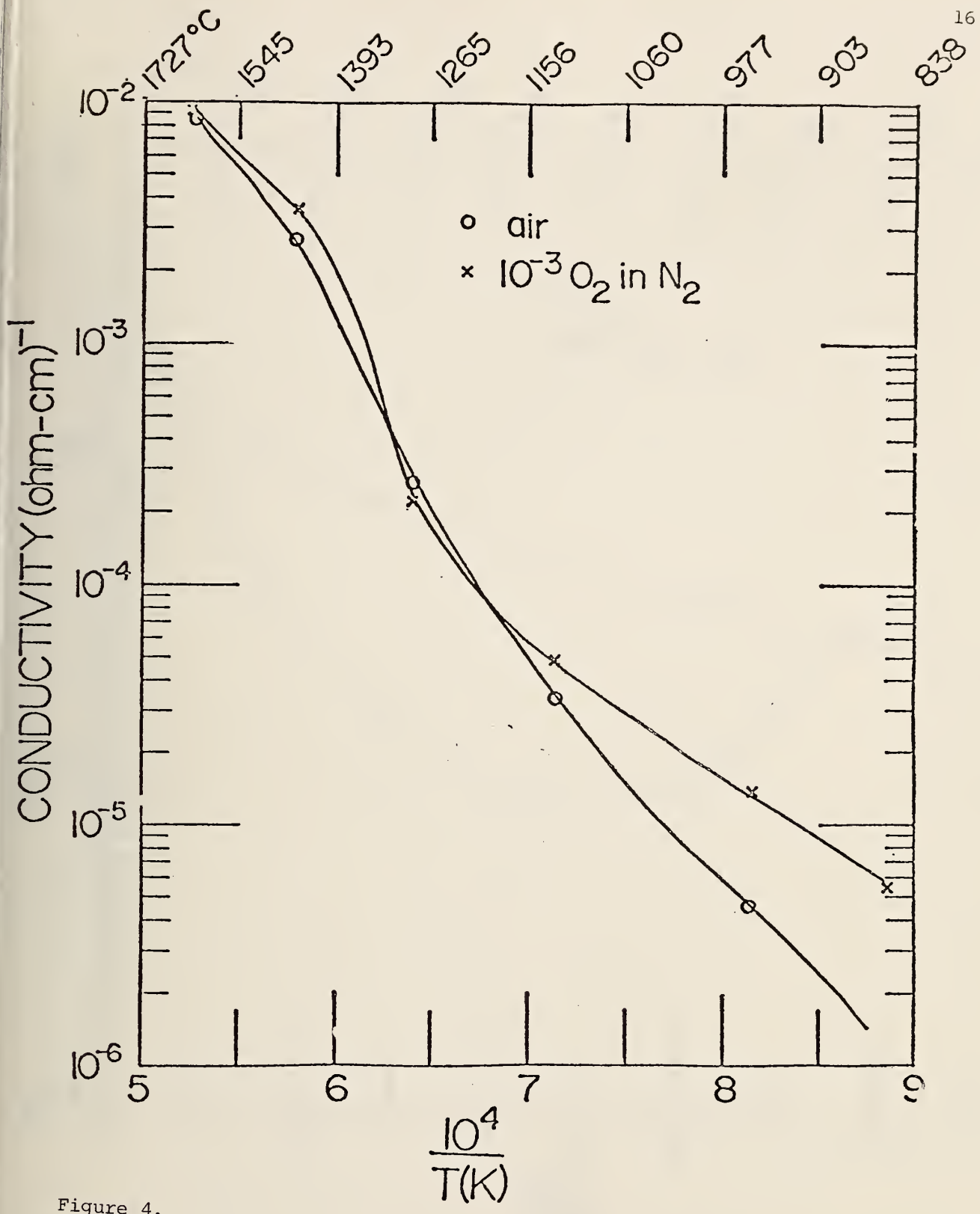

Figure 4.

Electrical conductivity of $Sr_{.97}La_{.02}ZrO_3$ as a function of temperature at several partial pressures of oxygen. Sample prepared by H. Anderson, A. T. Research. Measurements made at NBS.

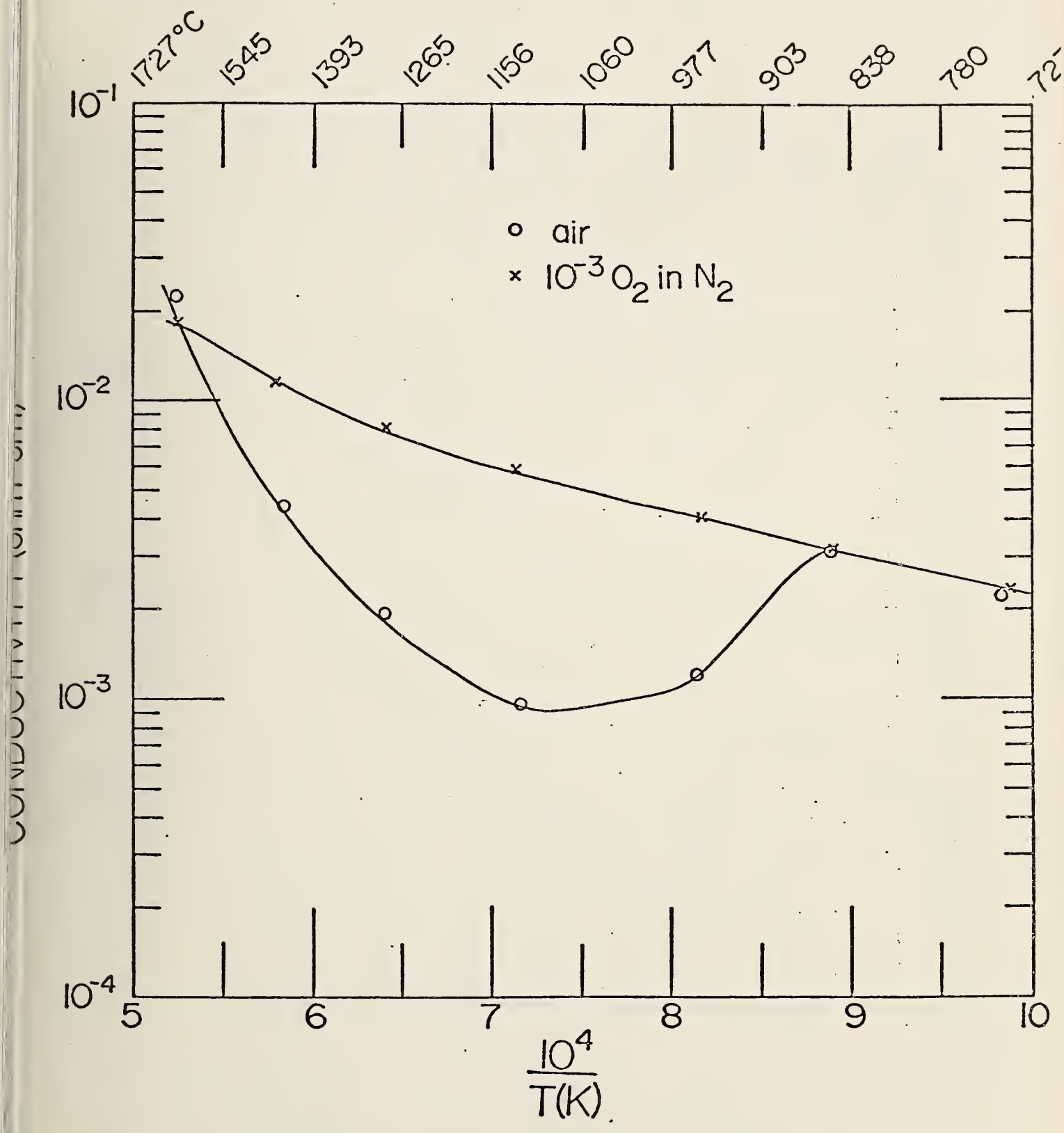

Figure 5.

Electrical conductivity of 0.9 ($SrZrO_3$) + 0.1 ($La_{.84}Sr_{.16}CrO_3$) as a function of temperature at several partial pressures of oxygen. Sample prepared by H. Anderson, AT Research. Measurements made at NBS.

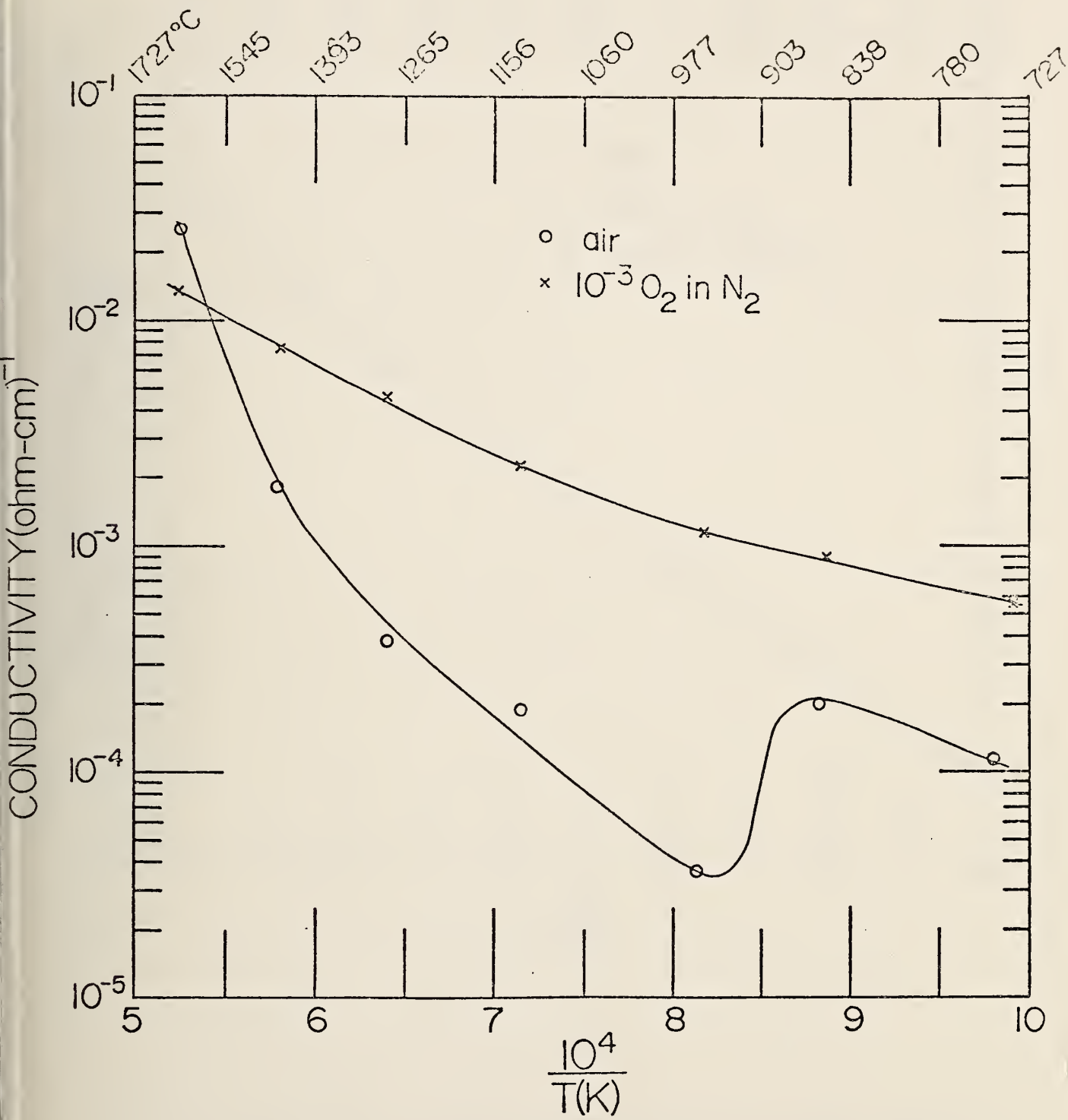

Figure 6. Electrical conductivity of $Sr_{.9}La_{.1}Zr_{.8}Cr_{.2}O_3$ as a function of temperature at several partial pressures of oxygen. Sample prepared at A T Research. No details on preparation were given.

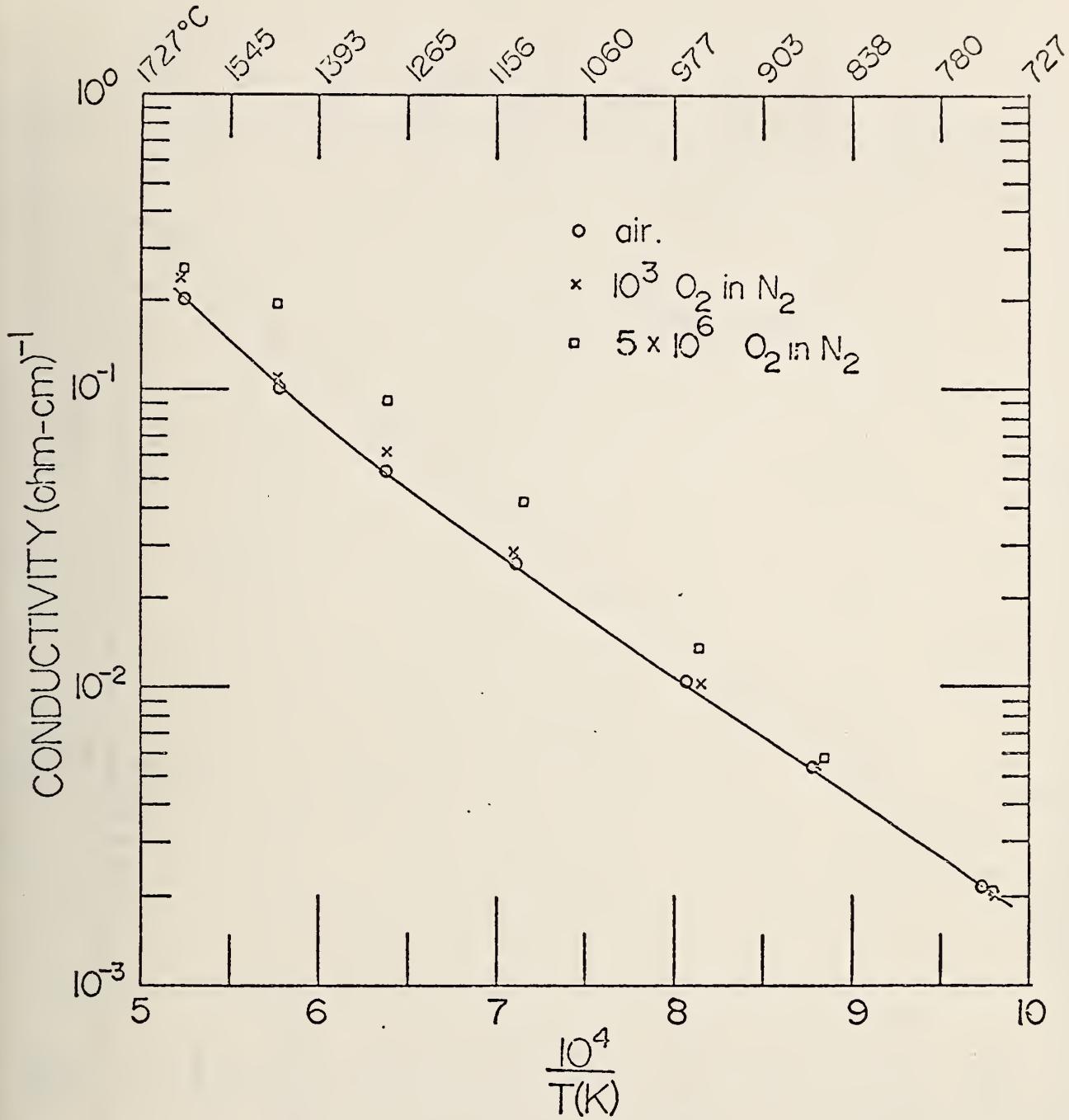

Figure 7.

Electrical conductivity of sintered $85ZrO_2$-$12CeO_2$-$3Y_2O_3$ (mole percent) as a function of temperature at several partial pressures of oxygen. Sample CZ--CE0101 from Westinghouse. Measurements made at NBS

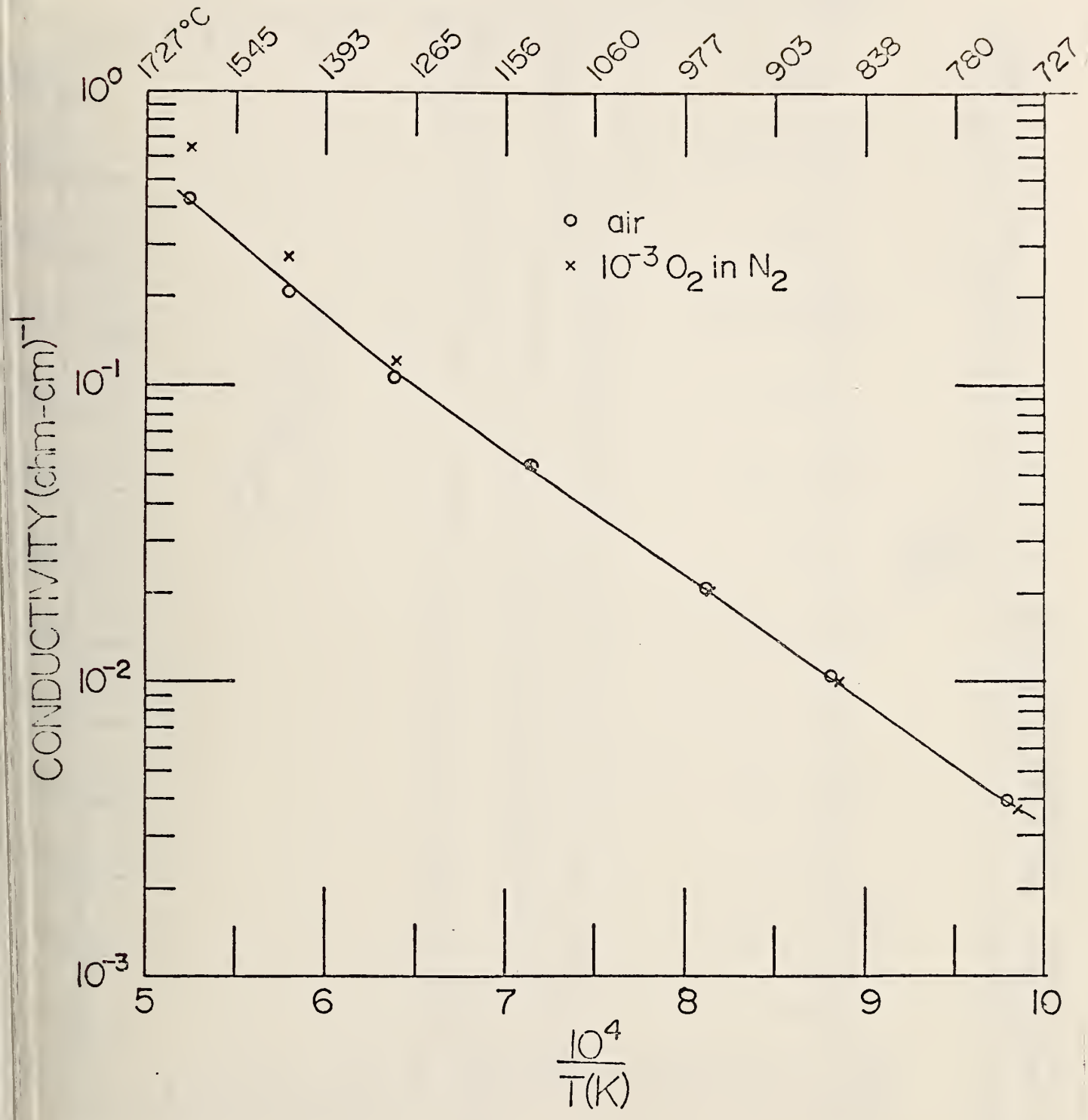

Figure 8. Electrical conductivity of 85 m/o ZrO_2-12 m/o CeO_2 -3 m/o Y_2O_3 as a function of temperature at several partial pressures of oxygen. This sample (CZ-CEO201) was made at Westinghouse and hot pressed at 1620 °C and 4000 psi.

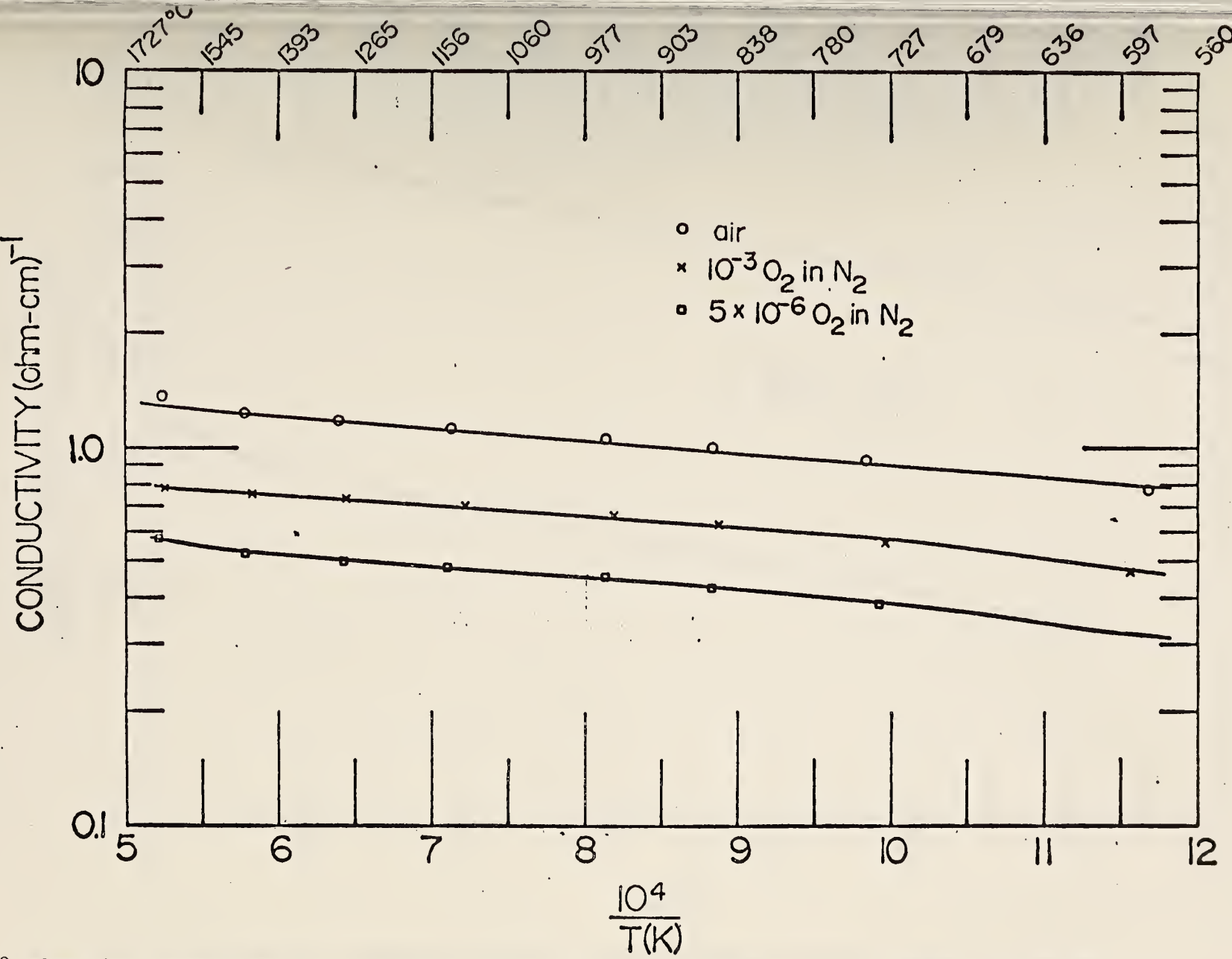

Fig. 9. Electrical conductivity of $La_{.95}Mg_{.05}CrO_3$ with 30 w/o of $88ZrO_2$ -12 Y_2O_3 added. Hot pressed at 1620 °C and 3000 psi. Room temperature conductivity in air is 1.63×10^{-2} $(ohm\ cm)^{-1}$. Sample made by Westinghouse. Measurements made at NBS.

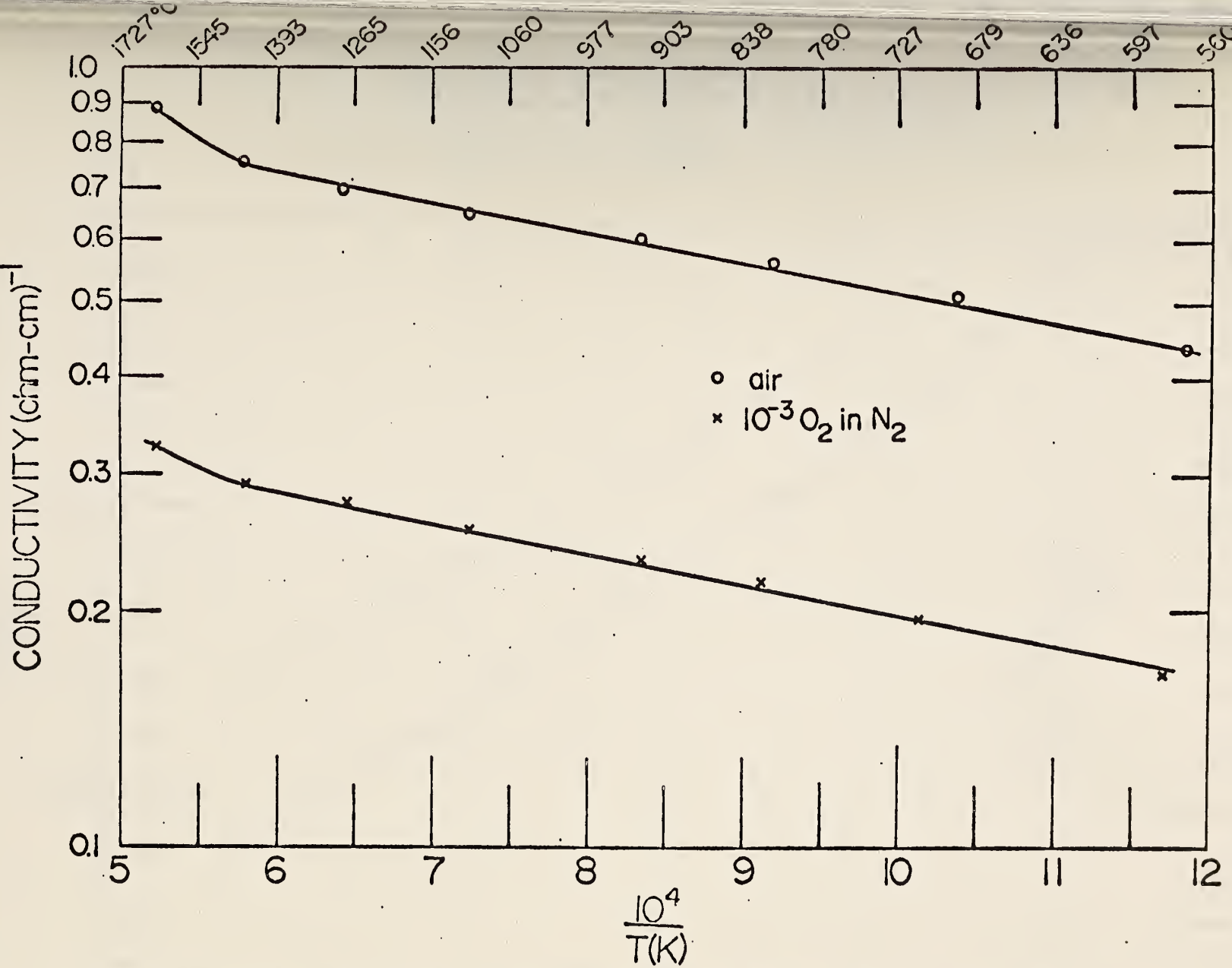

Fig. 10. Electrical conductivity of $La_{.95}Mg_{.05}CrO_3$ with 40 w/o ZrO_2 -12 Y_2O_3 added. Westinghouse sample LC-GR0603, hot pressed at 3000 psi and 1620 °C. Measurements made at NBS.

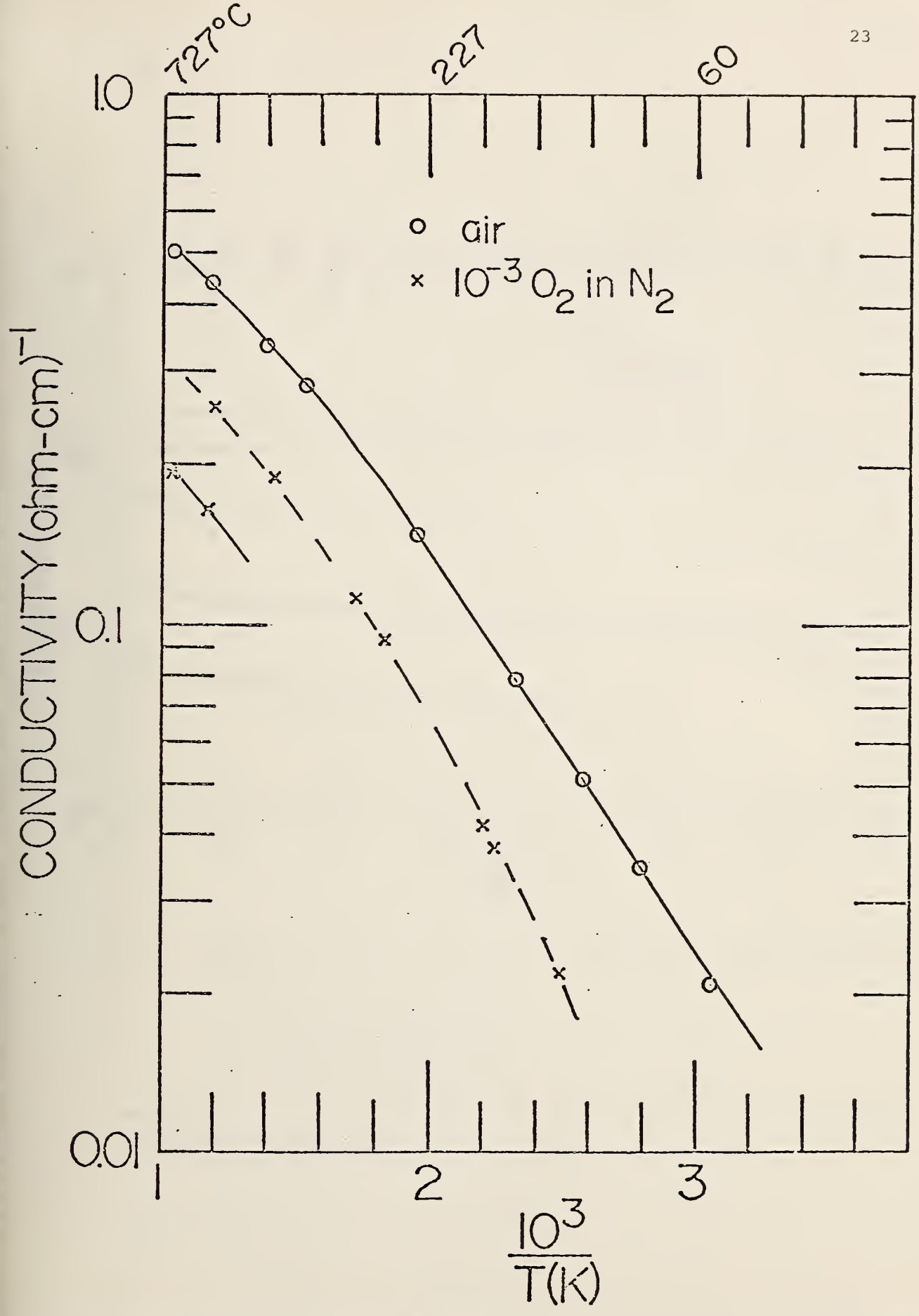

Fig. 11. Electrical conductivity of $La_{.95}Mg_{.05}CrO_3$ with 40 w/o ZrO_2-12Y_2O_3 added. Westinghouse sample LC-GRO603, hot pressed at 3000 psi and 1620 °C. Measurements made at NBS. The dashed line is data taken after the sample had been heated a second time to 1600 °C in 10^{-3} O_2 in N_2.

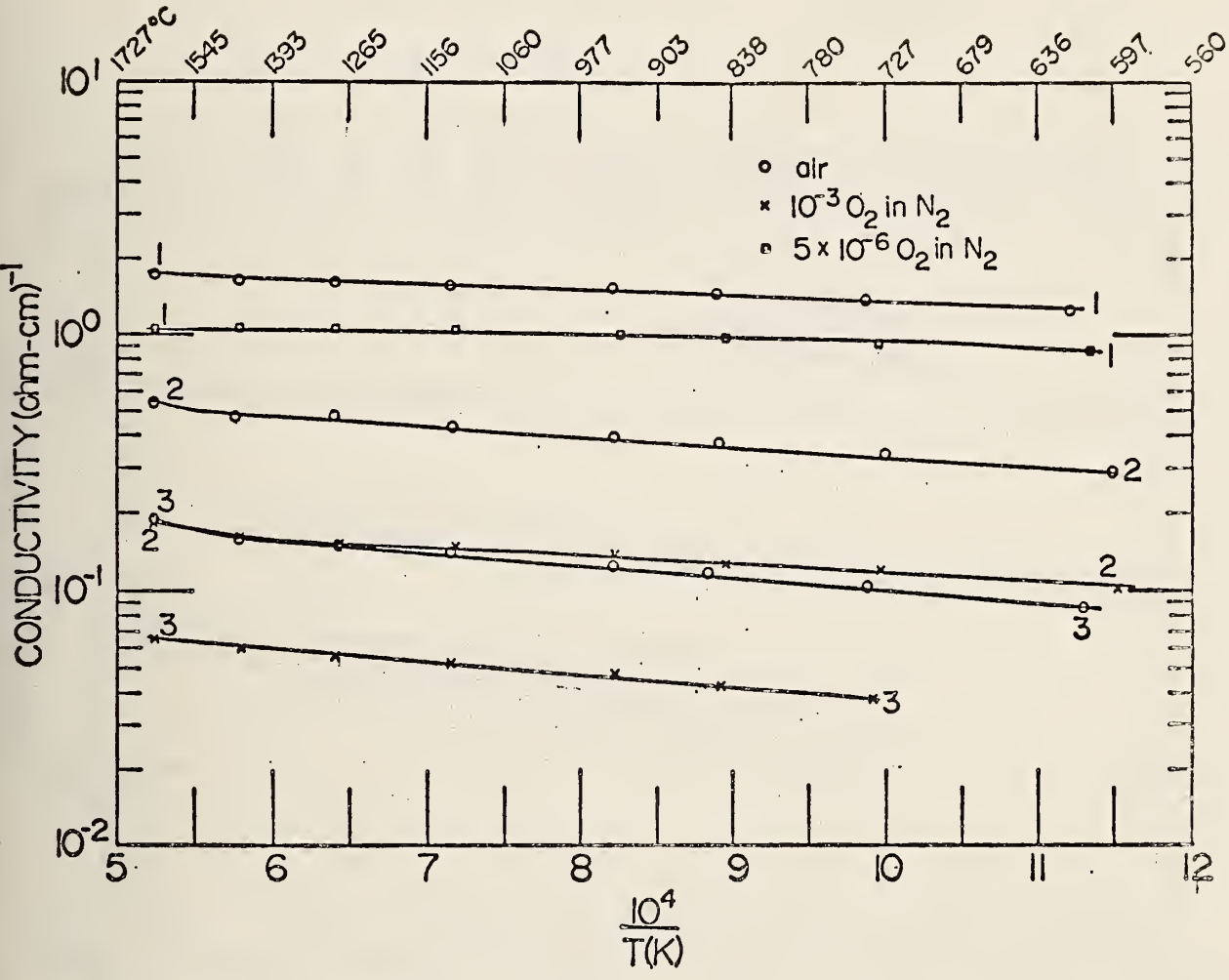

Figure 12. Electrical conductivity of hot pressed $La_{.95}Mg_{.05}CrO_3$ with added alumina.

1. $La_{.95}Mg_{.05}Cr_{.85}Al_{.15}O_3$
2. $La_{.95}Mg_{.05}Cr_{.68}Al_{.32}O_3$
3. $La_{.95}Mg_{.05}Cr_{.50}Al_{.50}O_3$

The samples were made at Westinghouse (pressed at 2000 psi and 1620 °C). Measurements made at NBS.

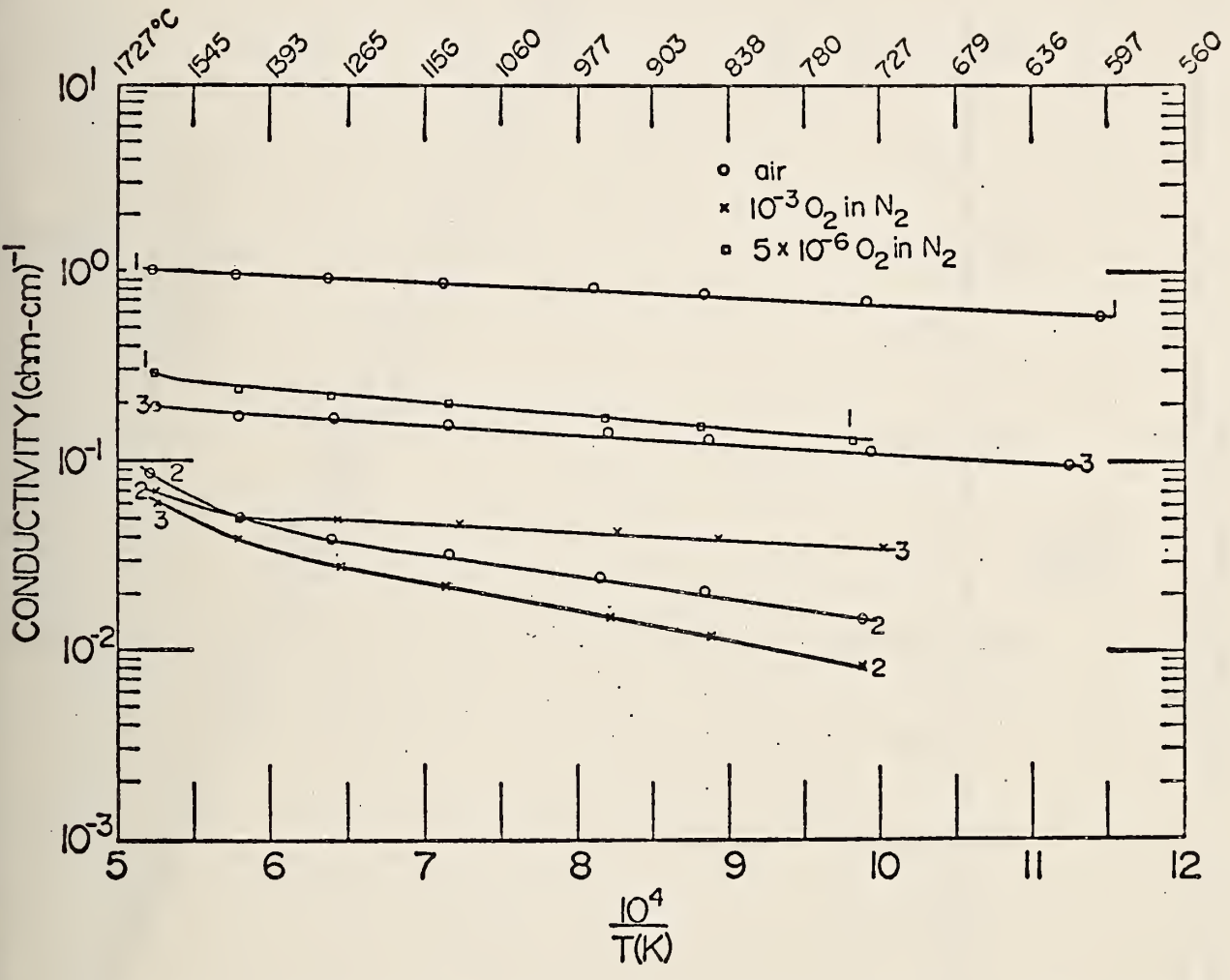

Figure 13. Electrical conductivity of sintered $La_{.95}Mg_{.05}CrO_3$ with added alumina.

1. $La_{.95}Mg_{.05}Cr_{.85}Al_{.15}O_3$
2. $La_{.95}Mg_{.05}Cr_{.68}Al_{.32}O_3$
3. $La_{.95}Mg_{.05}Cr_{.50}Al_{.50}O_3$

This sample was made by H. U. Anderson, A T Research. Measurements were made at NBS.

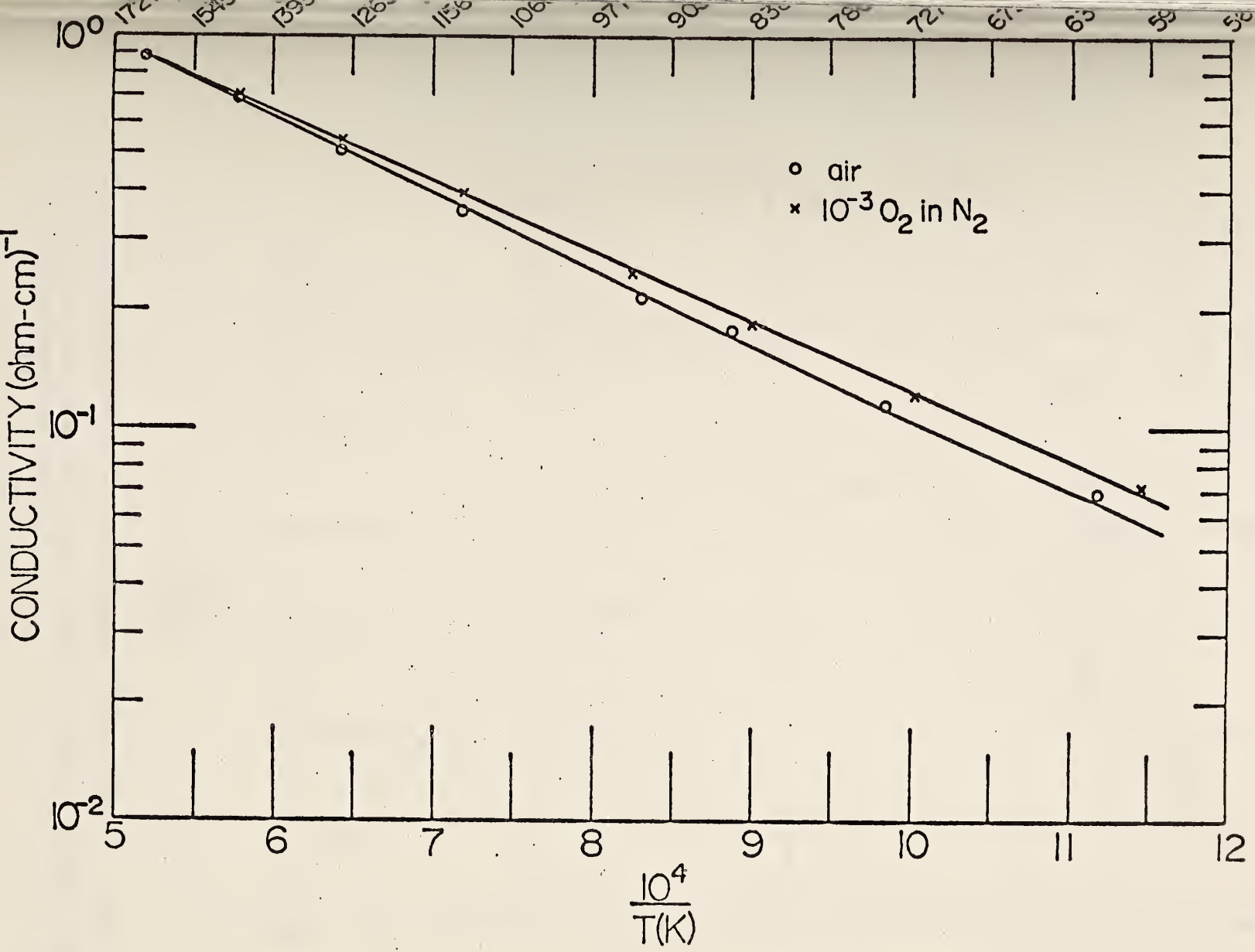

Fig. 14. Electrical conductivity of General Electric magnesium aluminate ferrous ferrite. Sample prepared by G.E. Measurements made at NBS.

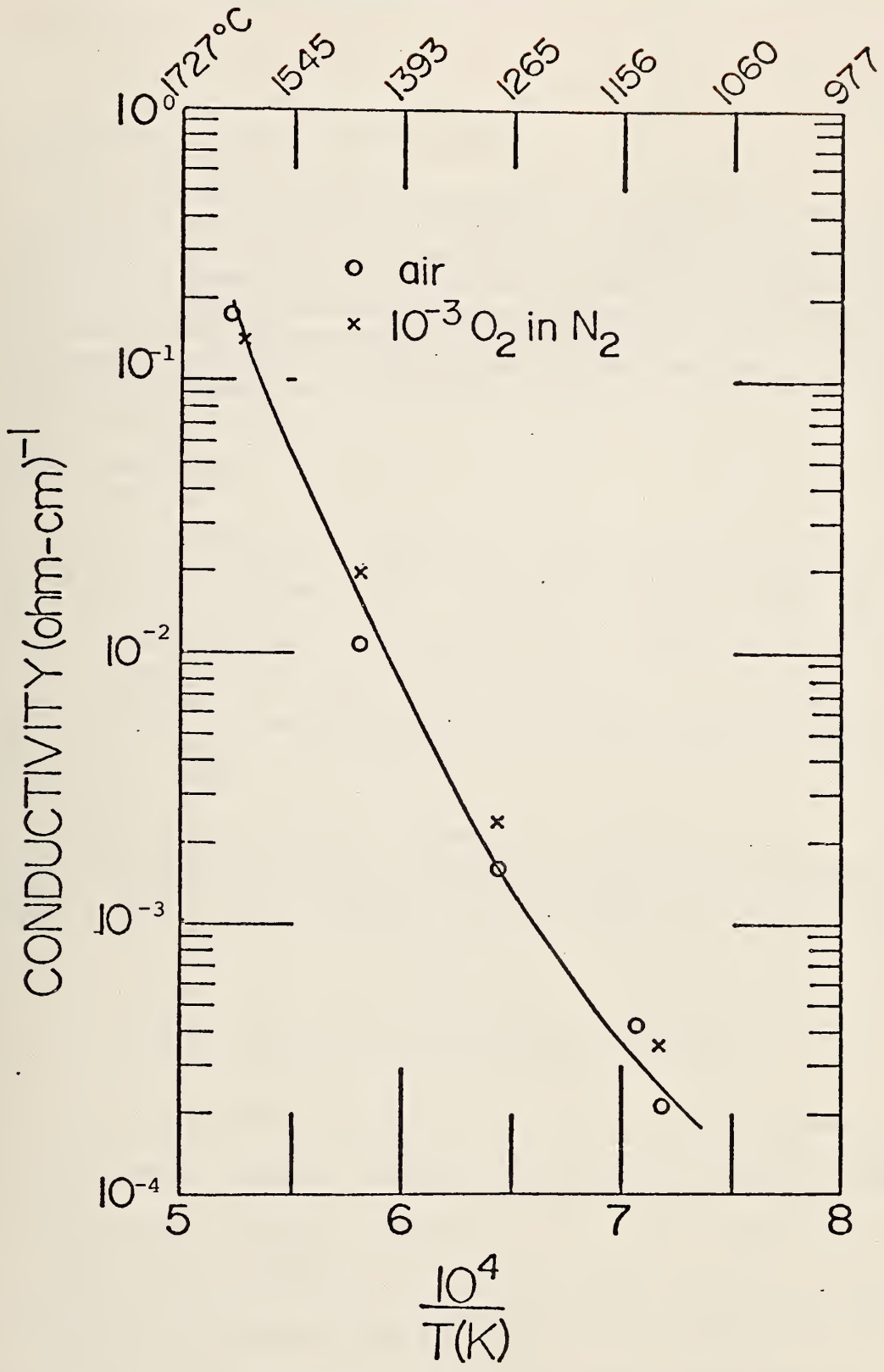

Fig. 15. Electrical conductivity of $82HfO_2$ - $18CeO_2$ (m/o). Sample T-1 hot pressed at 3500 psi and 1290 °C in argon. Sample made at ANL and measured at NBS.

3. Vaporization Studies (E. R. Plante)

This section describes measurements of the potassium gas pressure over K_2O-containing compounds or phases. Such data are of critical importance in predicting the interaction of a seeded MHD plasma with construction materials or coal ash using equilibrium thermodynamics. During this quarter measurements were completed on K_2SO_4(s) using the Mettler Microbalance System (in collaboration with C. Olson and T. Negas). Vaporization measurements were also made using the mass spectrometric technique on "$KFeO_2$" and several compositions in the K_2O-$A\ell_2O_3$-SiO_2 system.

K_2SO_4 Measurements

In the last quarterly report (1) details of results of the vaporization of K_2SO_4 were reported. During this quarter additional measurements on this system were completed. The purpose of this work was to confirm our previous measurements and to extend the temperature range over which data had been obtained. To accomplish this, measurements were made using a Knudsen cell having a 1mm diameter orifice in contrast to the 1/2mm diameter orifice used in the previous work. Other things being equal, this will increase the rate of mass loss from the effusion cell by a factor of 4, thus increasing the pressure range over which measurements can be made.

Analysis of the new data shows that it agrees very well with the results obtained previously. A summary of the second law heat of sublimation, third law heat of sublimation and entropy of sublimation at 298K using the 1/2mm and 1mm diameter effusion orifice is listed in table 2.

TABLE 2

Heats and Entropy of Sublimation of K_2SO_4(s)

		1mm effusion orifice	1/2mm effusion orifice
$\Delta H_s°$ (2nd)	(cal/mol)	80150 ± 930	81140 ± 1960
$\Delta H_s°$ (3rd)	(cal/mol)	81750 ± 40	81780 ± 60
$\Delta S_s°$ (2nd)	(gibbs/mol)	46.60 ± .90	45.82 ± 1.55
$\Delta S_s°$ (3rd)	(gibbs/mol)	45.313	45.313

The calculated third law heat of sublimation is from the work of Gurvich *et al* (2). Uncertainties are standard errors. This confirms our previous results which showed that the generally accepted saturation pressure of K_2SO_4 reported by Halstead (3) is too high by a factor of 5.

"$KFeO_2$" Measurements

These measurements were undertaken because iron is an important slag phase constituent as well as a possible electrode dopant. A sample of $KFeO_2$ provided by C. McDaniel was studied by mass spectrometry. The sample was contained in a Pt effusion cell having a .0135" diameter orifice and measurements of the $^{39}K^+$ and $^{32}O_2^+$ ion currents were made in the temperature range 900 - 1300° C. In air (P_{O_2} = .20 atm) the K_2O-Fe_2O_3 system is reasonably well characterized as a binary system up to about 1500° C but under the conditions of our experiment the O_2 pressure generated by the sample may be sufficient to cause changes in the sample composition. One can imagine the vaporization reaction to take place stepwise so that phases analogous to β alumina could be formed according to the following reaction sequence (compositions approximate);

$$7\ K_2O \cdot Fe_2O_3 = 2K(g) + 1/2O_2(g) + 6/7\ K_2O \cdot 7\ Fe_2O_3 \quad (1),$$

$$K_2O \cdot 7Fe_2O_3 = 2K(g) + 1/2O_2(g) + 7Fe_2O_3(s) \quad (2),$$

$$3Fe_2O_3(s) = 2Fe_3O_4(s) + 1/2O_2(g) \quad (3).$$

This reaction sequence will take place only if the O_2 pressure is sufficiently high to stabilize subsequent phases formed, for example, $K_2O \cdot 7Fe_2O_3$ and Fe_2O_3. X-ray analysis of the residue from the vaporization experiment showed the presence of a small amount of $KFeO_2$ and primarily the β" phase; a slightly reduced phase having the approximate composition $K_2O \cdot 7Fe_2O_3$. This data indicates that reaction (1) is the primary vaporization process. However, the mass spectrometric measurements were not entirely in accord with this interpretation because the oxygen pressure estimated from the measured I^+_{32} was about twice the potassium pressure. This would not be possible if the vaporization process is represented by reaction (1). It appears possible that the oxygen pressure may have been increased because of solution of Fe in the Pt cell from the $KFeO_2$ or $K_2O \cdot 7Fe_2O_3$ phases.

Because of this problem, the mass spectrometer calibration factor is uncertain by a factor of 3. Accepting the lower limit as the calibration factor, the calculated K pressures vary roughly from 10 times to twice as high as the K pressures over $KA\ell O_2$ at temperatures from 925 to 1300° C respectively.

These results are consistent with the idea that K_2O interacts less strongly with Fe_2O_3 than with $A\ell_2O_3$ or SiO_2 even though the K pressures may have been reduced because of excessive oxygen pressures.

K_2O-$A\ell_2O_3$-SiO_2 Measurements

These measurements are still in progress and will be reported on in more detail in forthcoming reports.

Future Work

During the next quarter measurements on the K pressure over K_2O-SiO_2-

Al_2O_3 solutions will be continued. Measurements on $KFeO_2$ in which the sample is not in contact with Pt will be attempted.

References

1. H. P. R. Frederikse, T. Negas, and S. J. Schneider, NBS Quarterly Report, June 1977.

2. L. V. Gurvich, O. V. Dorofeeva, and V. S. Yungman, Proceedings of the Conference on High Temperature Science Related to Open-Cycle, Coal-Fired MHD Systems, ANL-77-21 (1977).

3. W. D. Hafstead, Trans. Farad. Soc., 66, 1966 (1970).

Summary

Vapor pressures of K_2SO_4(c) using a 1 mm effusion orifice agreed with previous NBS measurements showing that the heretofore accepted measurements of Halstead are high by a factor of 5. Measurements of the K pressure over $KFeO_2$ are consistent with reduced stability of $KFeO_2$ as compared to $KAlO_2$.

1. Seed-Slag Interactions

a. Thermochemistry of the System $CaO-K_2O-Al_2O_3-SiO_2$ (L. P. Cook)

In the report for the preceding quarter, a working model for equilibrium subsolidus relations in the (Ca, Al, Si)-rich part of the seed/slag model system was given, based upon experimental data available at that time. Since then a series of long-duration crystallization experiments on seven synthetic calcium - containing slags has been completed (Table 1). These experiments were conducted as follows: roughly equal parts of well-characterized crystalline phases were weighed according to the proposed model and thoroughly mixed. These were then melted at 1610°C, quenched and subjected to 3 days, 1200°C crystallizations, followed by grinding, x-ray, and a two-week, 1200°C crystallization. Final products are shown in Table 1. On this basis, it appears that the equilibrium relations proposed are verified for the four-phase volumes: $Ca_2Al_2SiO_7$-$KAlSi_2O_6$-$KAlSiO_4$-$CaAl_2Si_2O_8$, $Ca_2Al_2SiO_7$-$KAlSi_2O_6$-$KAlSiO_4$-$CaSiO_3$, $Ca_2Al_2SiO_7$-$CaSiO_3$-$Ca_2Al_2Si_2O_8$-$KAlSi_2O_6$, and Al_2O_3-$CaAl_2Si_2O_8$-$KAlSiO_4$-$KAlSi_2O_6$ at 1200°C (Figure 1). This temperature is not far from the temperature of minimum melting for these volumes and the use of these assemblages in calculating potassium pressures is warranted. Owing to the difficulty in crystallizing the incongruently-melting compounds $CaAl_{12}O_{19}$ and $3Al_2O_3 \cdot 2SiO_2$ complete reversibility of melting experiments was not obtained at 1200°C for the four-phase volumes $CaAl_{12}O_{19}$-$CaAl_2Si_2O_8$-Al_2O_3-$KAlSiO_4$, $CaAl_{12}O_{19}$-$Ca_2Al_2SiO_7$-$CaAl_2Si_2O_8$-$KAlSiO_4$, and $3Al_2O_3 \cdot 2SiO_2$-Al_2O_3-$CaAl_2Si_2O_8$-$KAlSi_2O_6$. However no reactions occurred which would indicate disequilibrium within these four phase volumes as proposed. Additional slag crystallization experiments, at higher temperatures, are planned for definitive verification of assemblages.

As noted in the previous quarterly report, thermochemical calculations gave log $(P_K^2 \cdot P_{O_2}^{1/2})$ vs T curves for invariant melts from four-phase volumes. These curves plotted in relative positions at variance with those predicted from equilibrium topologies. Preliminary calculations indicate that approximately 20 mole % substitution of $KCaAlSi_2O_7$ in $Ca_2Al_2SiO_7$ (see reactions 2-b, 3-b, 4-b, 7-b in preceding quarterly report, Table 1, p. 43) would alter the positions of these curves so that they fall nearly in the order predicted, within the uncertainties of the thermochemical data. The first step in the experimental approach to this problem is determination of the solubility of K_2O in gehlenite and relation of this to its x-ray properties. Unfortunately the results of Nurse and Midgeley [1] have proved impossible to duplicate. A similar problem has been encountered by Yoder [2] in his work on sodium solubility in $Ca_2Al_2SiO_7$. There are indications that low temperature decomposition may be the explanation, and further experimentation must utilize high-temperature x-ray apparatus. This has caused an unexpected, though hopefully not serious, delay in the completion of milestone 17-a.

Additional experiments have been conducted in the system to determine the compatibility of K_2CaSiO_4 with $KAlO_2$-SiO_2 compounds (Table 2). This compound (mp ~1610°) has been postulated as structurally related to $KAlO_2$ [3], possible only if a relationship of the form $CaSi \rightleftarrows AlAl$ holds; this is not likely as it would require Ca in tetrahedral coordination. X-ray analysis of $K_2CaSiO_4/KAlO_2$ mixtures equilibrated at 1200°C for two weeks suggests intermediate phases. On the other hand, as data in Table 2 show, K_2CaSiO_4 and $KAlSi_2O_6$ react extensively to form melt at 1200°C. K_2CaSiO_4 and $KAlSiO_4$ react in an undetermined way with extensive formation of tetragonal $K_{1+x}Al_{1+x}Si_{1-x}O_4$-type solid solution.

Various substitutional possibilities involving calcium will be further investigated under Milestone 21.

References

1. R.W. Nurse and H.G. Midgley, 1953, J. Iron and Steel Inst. 174, 121-131.

2. H.S. Yoder, 1973, Fortschr. Miner. 50, 140-173.

3. H. Hughes, 1966, Trans. Brit. Ceram. Soc. 65, 661-679.

Table 1. Crystallization Experiments on Synthetic CaO-Containing Slags.

Four Phase Mixture[a]	Heat Treatment (Approx. Times) Initial T(°C)	Hr	Final T(°C)	Hr	X-ray Diffraction Analysis of Products
Kℓs/Cor/CA_6/An	1610[b]	0.25			
	1200[c]	70			Cor + Glass
			1200[c]	335	Kℓs + Cor + An + Glass(?)
Kℓs/CA_6/Ge/An	1610[b]	0.25			
	1200[c]	70			CA_6 + Ge + Glass
			1200[c]	335	Kℓs + CA_6 + Ge + An
Kℓs/Lc/Ge/An	1610[b]	0.25			
	1200[c]	70			Glass
			1200[c]	335	Kℓs + Lc + Ge + An
Kℓs/Lc/Ge/Wo	1610[b]	0.25			
	1200[c]	70			Kℓs + Glass
			1200[c]	335	Kℓs + Lc + Ge + Wo
Kℓs/Lc/Cor/An	1610[b]	0.25			
	1200[c]	70			Lc + Cor + Glass
			1200[c]	335	Kℓs + Lc + Cor + An
Lc/Cor/Mu/An	1610[b]	0.25			
	1200[c]	70			Lc + Cor + An + Glass
			1200[c]	335	Lc + Cor + An + Glass(?)
Lc/Ge/An/Wo	1610[b]	0.25			
	1200[c]	70			Glass
			1200[c]	335	Lc + Ge + An + Wo

[a] Kℓs = $KAlSiO_4$
Cor = Al_2O_3
CA_6 = $CaAl_{12}O_{19}$
An = $CaAl_2Si_2O_8$
Ge = $Ca_2Al_2SiO_7$
Lc = $KAlSi_2O_6$
Wo = $CaSiO_3$

[b] Quenched in water

[c] Air Cooled

Table 2. Compatibility of K_2CaSiO_4 with $KAlO_2$-SiO_2 Based Materials.

Starting Materials	Heat Treatment (Approx. Time) T(°C)	Hr	X-ray Diffraction Analysis of Products (Tentative Identification)
K_2CaSiO_4 + $KAlO_2$	1200[a/]	335	K_2CaSiO_4 + $KAlO_2$(ss) + intermediate (ss) (?)
K_2CaSiO_4 + $KAlSiO_4$	1200[a/]	335	$K_{1+x}Al_{1+x}Si_{1-x}O_4$ + $KAlO_2$(ss) + K_2CaSiO_4
K_2CaSiO_4 + $KAlSi_2O_6$	1200[a,b/]	335	Glass

a/ Air cooled

b/ Capsule burst

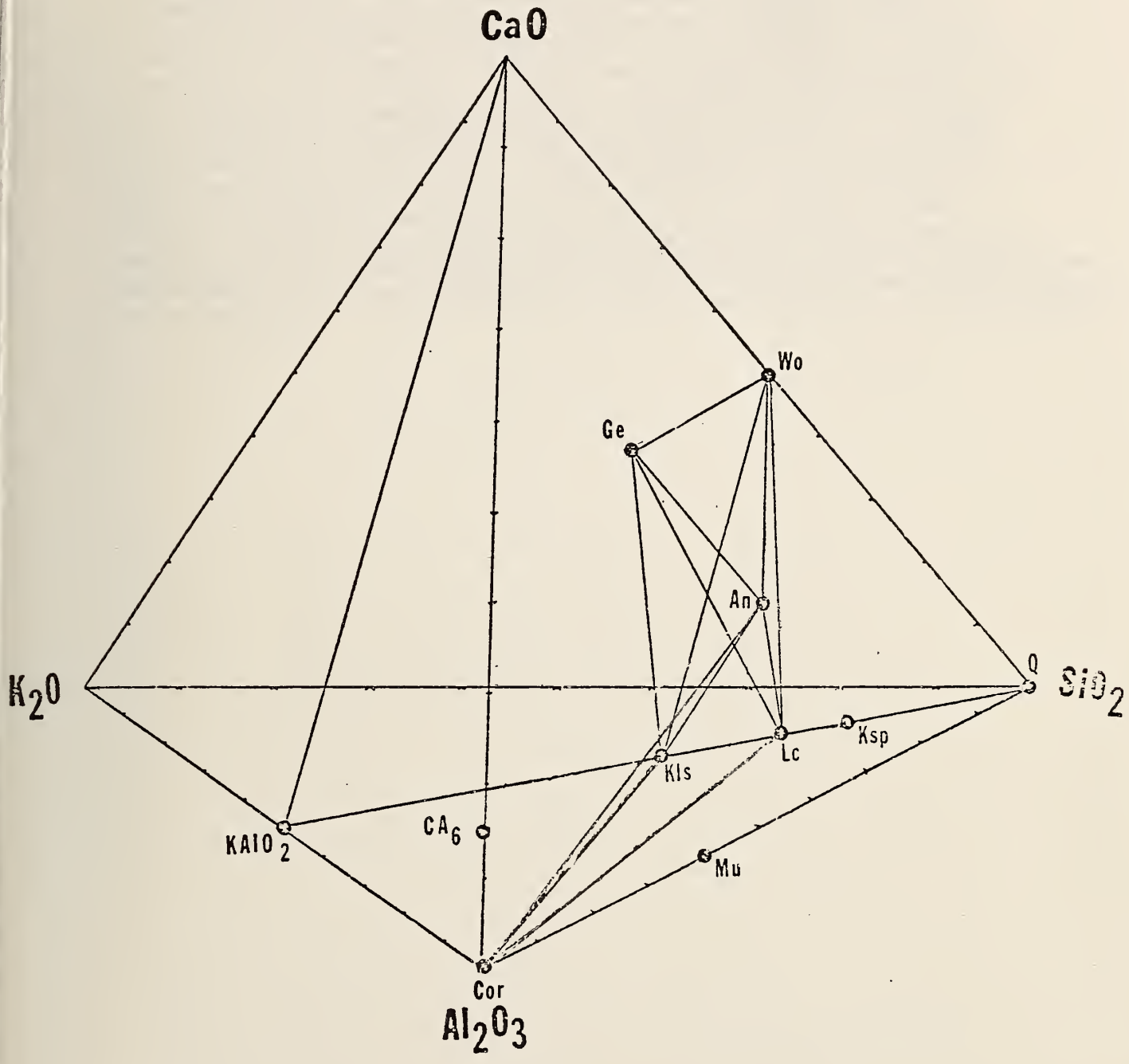

Figure 1. Four-phase equilibrium volumes in the system $CaO-K_2O-Al_2O_3-SiO_2$, as verified by synthetic slag crystallization experiments at 1200°C. Abbreviations as in Table 1.

Thermochemistry of the System $MgO-K_2O-Al_2O_3-SiO_2$ (L. P. Cook)

A series of long duration crystallization experiments on four synthetic magnesium-containing slags has been completed (Table 3). These experiments were conducted in a manner analogous to those conducted in the calcium containing system. Final products are shown in Table 3. On this basis, it appears that the equilibrium relations are verified for the four-phase volumes: $Al_2O_3-MgAl_2O_4-KAlSiO_4-KAlSi_2O_6$ and $Mg_2SiO_4-MgAl_2O_4-KAlSiO_4-KAlSi_2O_6$ at 1200°C (Figure 2). Owing to the difficulty in crystallizing the incongruently melting compounds $3Al_2O_3 \cdot 2SiO_2$ and $Mg_2Al_4Si_3O_{18}$, complete reversibility of melting experiments was not obtained at 1200°C for the four-phase volumes: $3Al_2O_3 \cdot 2SiO_2-MgAl_2O_4-KAlSi_2O_6-Al_2O_3$ and $Mg_2Al_4Si_5O_{18}-KAlSi_2O_6-MgAl_2O_4-Mg_2SiO_4$. However no reactions occurred which would indicate disequilibrium within these four-phase volumes as proposed. Additional slag crystallization experiments, at higher temperatures, are planned for definitive verification of assemblages.

Table 3. Crystallization Experiments on Synthetic MgO-Containing Slags.

Four Phase Mixture[a]	Heat Treatment (Approx. Time) Initial T(°C)	Initial Hr	Final T(°C)	Final Hr	X-ray Diffraction Analysis of Products
Cd/Lc/Sp/Fo	1610[b]	0.25			
	1200[c]	70			Fo + Sp + Glass
			1200[c]	335	Fo + Sp + Lc + Glass (?)
Cor/Sp/Kℓs/Lc	1610[b]	0.25			
	1200[c]	70			Cor + Sp + Kℓs + Lc
			1200[c]	335	Cor + Sp + Kℓs + Lc
Fo/Sp/Kℓs/Lc	1610[b]	0.25			
	1200[c]	70			Fo + Sp + Kℓs + Glass
			1200[c]	335	Fo + Sp + Kℓs + Lc
Cor/Lc/Sp/Mu	1610[b]	0.25			
	1200[c]	70			Cor + Sp + Glass
			1200[c]	335	Cor + Sp + Lc + Glass (?)

[a] Cd = $Mg_2Al_4Si_5O_{18}$
Lc = $KAlSi_2O_6$
Sp = $MgAl_2O_4$
Fo = Mg_2SiO_4
Kℓs = $KAlSiO_4$
Mu = $3Al_2O_3 \cdot 2SiO_2$

[b] Quenched in water

[c] Air cooled

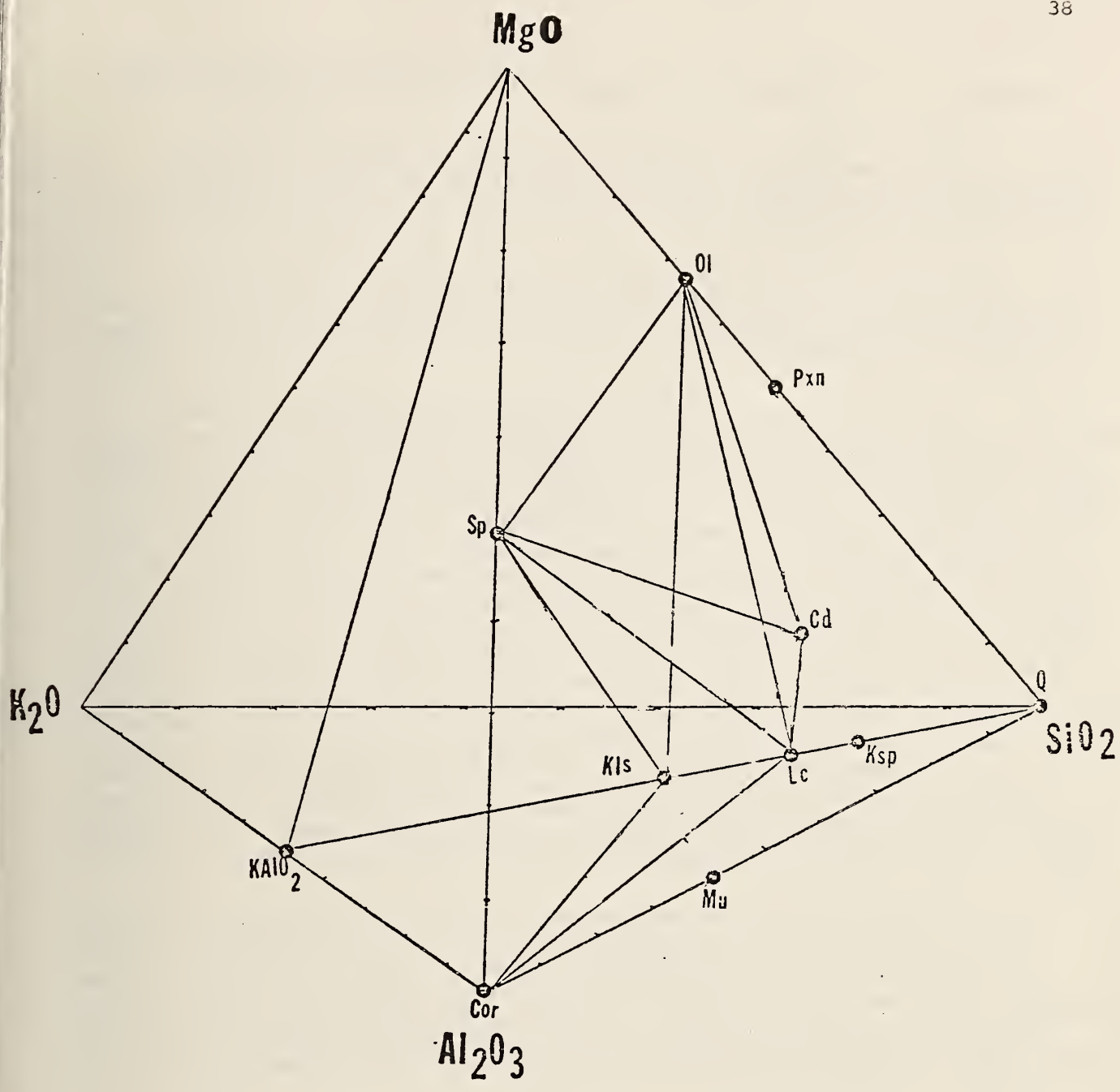

Figure 2. Four-phase equilibrium volumes in the system $MgO-K_2O-Al_2O_3-SiO_2$, as verified by synthetic slag crystallization experiments at 1200°C. Abbreviations as in Table 3.

2. Diffusion in Insulator-Electrode Couples (A. J. Armstrong, E. N. Farabaugh and J. R. Manning

Work has continued on the study of insulator-electrode diffusion couples. Fe concentration profiles for the MAFF-MgO type couples have been determined for the case of 100 hr., 10 hr. and 1 hr. tests conducted at 1600 °C. These profiles are shown in Fig. 3.

A profile for the 10 hr. test was reported in the June 1977 report. The profile for the 10 hr. test shown in Fig. 3 is another set of data points taken from the same specimen which does essentially reproduce the previously reported profile.

There are several points that the profiles of Fig. 3 illustrate. Although there was a small gap between the MAFF and MgO (caused by the platinum wire boundary marker), the Fe profile follows rather smoothly from the MAFF to MgO. The gap hasn't caused any obvious changes in the profile. This was also noted in an earlier report. It is observed that a hump in the Fe profile appears only for the 10 hr. test. There is no explanation for this at present. The 100 hr. test diffused so much Fe into the MgO that the tails from the profile from opposite interfaces overlapped, prohibiting the Fe profile to go to zero in the MgO. The 1 hr. and 10 hr. runs show maximum penetrations proportional to $t^{1/2}$, as expected for diffusion processes. All the couples were scanned across the complete couple sandwich (MAFF-MgO-MAFF), i.e., data was taken in the MAFF, across the MgO and into the opposite slice of MAFF. This data showed that the profiles at the two MgO-MAFF interfaces for each sandwich were essentially the same. Only one interface is shown in the accompanying figure because of this reproducibility. Data for Mg and Al concentration profiles were recorded simultaneously with the Fe data for these couples. Although not shown in this report, these profiles indicated little diffusion of Al from the MAFF into the MgO and similarly little movement of Mg between the MAFF and MgO.

The profiles shown in Fig. 3 also indicate that the diffusion of Fe is faster in the MgO than the MAFF as evidenced by the larger penetration of Fe into the MgO as compared to depth of depletion of Fe in the MAFF for a specific test time. Preliminary analysis of these data indicate that diffusion coefficients can be determined for the 1 hr. and 10 hr. tests. In the case of the 100 hr. test, the overlapping of the profiles from opposite edges introduces some question to the usefulness of the test in obtaining a diffusion coefficient.

These data will be treated in the same manner as the case for K diffusion into Al_2O_3. We will assume a constant diffusion coefficient, D, in an infinite linear system obeying Fick's second law for a one-dimensional case. The data will be plotted on probability paper to yield D. These results will be given at the end of the next reporting period.

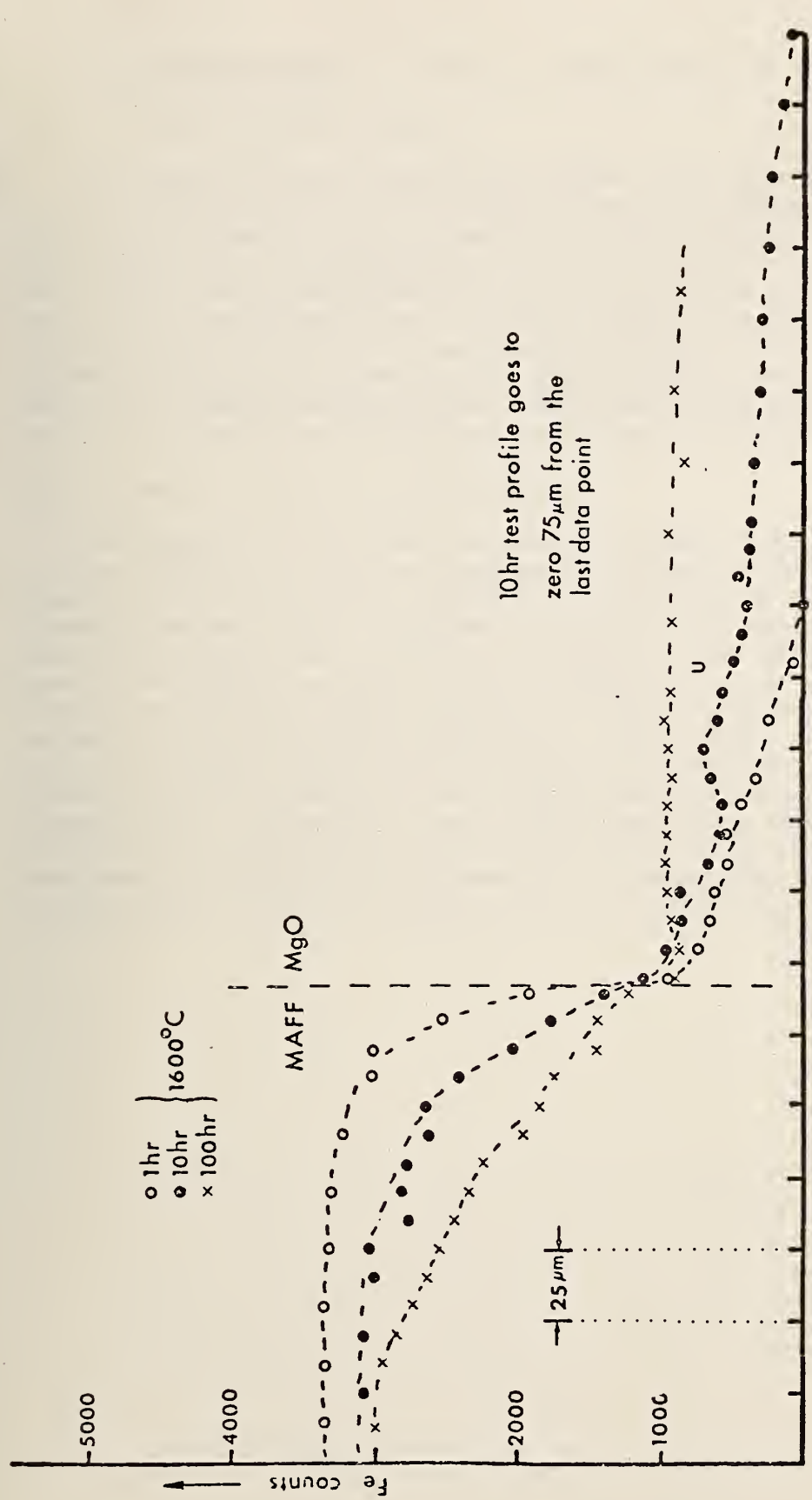

Figure 3. Fe concentration profiles for 1, 10 and 100 hr. test of MAFF-MgO-MAFF diffusion couple at 1600 °C.

3. Electrode Materials (C. Skarda, T. Negas and R. S. Roth)

a. The Ta_2O_5-CeO_x-FeO_x System

The Ta_2O_5-CeO_x-FeO_x system was explored, 1300-1550 °C in air (see Figure 4), to determine whether new mixed oxide phases having potentially desirable electrical properties can be prepared. Under oxidizing conditions two phases were found within the composition triangle (Fig. 4). Phase b has a homogeneity region only partly delimited thus far. The material is particularly interesting as it has a "pyrochlore-like" structure similar to many conducting rare-earth oxide/zirconia materials. Phase relations involving the b phase have not been sorted completely as oxidation-reduction (probably involving both Fe^{3+}/Fe^{2+} and Ce^{4+}/Ce^{3+}) complicate equilibria. Electrical measurements for this material will be initiated once an optimum composition is selected.

b. Potassium Ferrite (β-alumina-type)

As suggested in the previous Quarterly Report, K-ferrite having the β-alumina structure type have more than adequate electrical conductivity (mainly electronic) to be considered for usage as low temperature (<1400 °C) construction materials. Reactive powders (∿100 g) were prepared to provide starting materials for fabrication of specimens via hot-pressing. Several runs under varying conditions were conducted for us by Naval Research Labs. (NRL). The starting bulk composition was $K_2O{:}7(Fe_{1.9}Ti_{0.1}O_3)$; TiO_2 added to enhance the electrical conductivity. Single-phase, homogeneous products were not obtained from these preliminary hot-pressings. Rather than utilizing reactive starting powders, single phase K-ferrite powders will be used in future work. This requires some special handling of starting materials, and initially calcined powders together with appropriate control of the gaseous environment to maintain stoichiometry. In cooperation with a private firm these powders, hopefully suitable for hot-pressing, are being prepared.

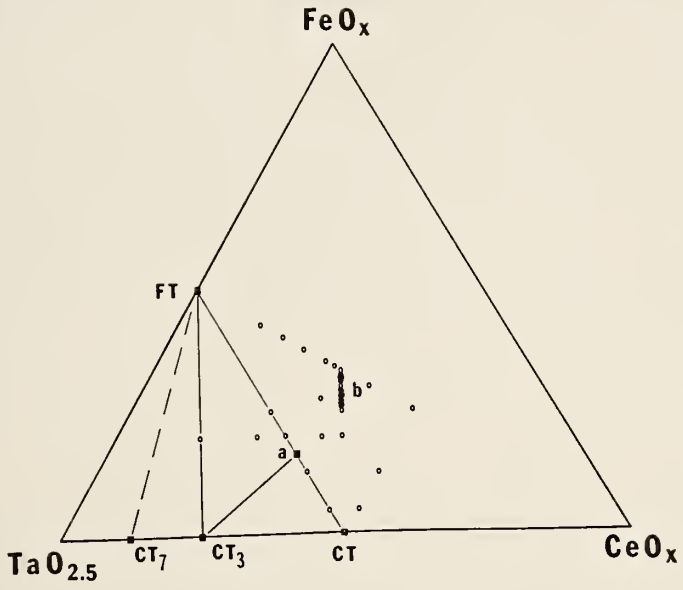

Figure 4. Projection of system Ta_2O_5-cerium oxide-iron oxide in air. 1300-1400°C. Open circles are bulk compositions investigated. FT = $FeTaO_4$ (rutile-type); CT_3 = $CeTa_3O_9$ (perovskite-type); CT = $CeTaO_4$; a = compound, $2CeTaO_4:FeTaO_4$ and b = homogeneity region, of a mixed oxide having a pyrochlore-like structure. Compositions plotted in terms of mol % of components as indicated without specific oxygen content (e.g. FeO_x = $FeO_{1.5}(Fe_2O_3)$, $FeO_{1.33}(Fe_3O_4)$, etc.; CeO_x = CeO_2, $CeO_{1.5}$, etc.).

TASK K. Materials Testing and Characterization

1. Structural Analysis of Powdered and Solid Ceramics

a. X-ray Diffraction of MHD Materials (C. L. McDaniel)

During this quarter we received about 60 materials (powders, dense ceramics, etc.) from various external sources. These were analyzed by x-ray diffraction methods. Data, transmitted to the appropriate source, are shown in Table 1.

Material	From	Description	Xray Diffraction
$La_{.95}Mg_{.05}CrO_3$	Trans-Tech	Powder - 1300°C 10 hrs	$LaCrO_3$ type phase - good crystallinity
$Y_{.95}Mg_{0.5}CrO_3$	Trans-Tech	Powder - 1300°C 12 hrs	$YCrO_3$ type phase - good crystallinity
$LaCrO_3$ + layer slag	NBS	Solid electrode	Amorphous to x-rays
$3MgAl_2O_4$-Fe_3O_4	NBS	Solid electrode	$MgAl_2O_4$ type phase - poor crystallinity
$MgAl_2O_4$	Trans-Tech	Solid	$MgAl_2O_4$ - very good crystallinity
$SrZrO_3$ (SZ-UM0101)	Westinghouse	Solid	$SrZrO_3$ + ∿5% tetragonal ZrO_2 + trace monoclinic ZrO_2 - very good crystallinity
$85ZrO_2$-$12CeO_2$-$3Y_2O_3$ (CZ-CE0101)	Westinghouse	Solid	At least two cubic (fluorite type) phases and/or tetragonal ZrO_2 - very poor crystallinity
$3MgAl_2O_4$-Fe_3O_4 LV11 44	Technetics	Solid	$MgAl_2O_4$ type phase + trace FeO - poor crystallinity
$LaMgCrO_3$	Trans-Tech	Powder - 1305°C 10 hrs	$LaCrO_3$ type phase - medium to good crystallinity
$La_{.95}Mg_{.05}CrO_3$	Trans-Tech	Powder - 1300°C 13 hrs	$LaCrO_3$ type phase - medium to good crystallinity
$3MgAl_2O_4$-Fe_3O_4 (3-1-R)	Trans-Tech	Powder	$MgAl_2O_4$ type phase - medium crystallinity
$MgAl_2O_4$ (4-1R)	Trans-Tech	Powder	$MgAl_2O_4$ - good crystallinity
$SrZrO_3$ #1	Trans-Tech	Powder	$SrZrO_3$ + 5-10% monoclinic ZrO_2 + ∿5% $Sr_4Zr_3O_{10}$ - medium crystallinity
Al_2O_3	Trans-Tech	Solid	Al_2O_3 - good crystallinity
Al_2O_3	Trans-Tech	Solid	Al_2O_3 - good crystallinity
$La_{.95}Mg_{.05}CrO_3$ LC-CE01PS	Westinghouse	Received as solid, powder prepared	$LaCrO_3$ type phase + ∿5% unknown phase, medium crystallinity
$La_{.95}Mg_{.05}CrO_3$ LC-CE01PSF	Westinghouse	1650°C 2 hr., received, as solid, powder prepared	$LaCrO_3$ type phase + ∿5% unknown phase, medium to good crystallinity

$La_{.95}Mg_{.05}CrO_3$ LC-CE02PSF	Westinghouse	1650°C 2 hr., received as solid, powder prepared	$LaCrO_3$ type phase + ∿5% $La(OH)_3$ - good crystallinity
$La_{.95}Mg_{.05}CrO_3$ LC-CE03	Westinghouse	Powder	$LaCrO_3$ type phase - medium crystallinity
$La_{.95}Mg_{.05}CrO_3$ #2	Trans-Tech	Powder	$LaCrO_3$ type phase - good crystallinity
$85ZrO_2$-$12CeO_2$-$3Y_2O_3$ 6751-A-2	CERAC	Powder	At least two cubic (fluorite type) phases + 1-5% monoclinic ZrO_2 - poor crystallinity
$LaCrO_3$ + MgO 71107-4	APS Mat. Co.	Received as solid, powder prepared	$LaCrO_3$ type phase, + ∿5% unknown phase, medium to good crystallinity
$LaCrO_3$ + MgO 71107-6	APS Mat. Co.	Received as solid, powder prepared	$LaCrO_3$ type phase + ∿5% unknown phase, medium to good crystallinity
$LaCrO_3$ + MgO 71107-5	APS Mat. Co.	Received as solid, powder prepared	$LaCrO_3$ type phase + ∿5% unknown phase, medium to good crystallinity
$MgAl_2O_4$ 71107-7	APS Mat..Co.	Received as solid, powder prepared	$MgAl_2O_4$ - medium to good crystallinity
$3MgAl_2O_4$-Fe_3O_4 71107-3	APS Mat. Co.	Received as solid, powder prepared	$MgAl_2O_4$ type phase - poor crystallinity
$3MgAl_2O_4$-Fe_3O_4 71107-1	APS Mat. Co.	Received as solid, powder prepared	$MgAl_2O_4$ type phase - poor crystallinity
$3MgAl_2O_4$-Fe_3O_4 71107-2	APS Mat. Co.	Received as solid, powder prepared	$MgAl_2O_4$ type phase - poor crystallinity
$9MgAl_2O_4$-Fe_3O_4 + Fe	Trans-Tech	Powder, 1000°C	$MgAl_2O_4$ type phase + ∿10% Fe_2O_3 - good crystallinity
$9MgAl_2O_4$-Fe_3O_4	Trans-Tech	Powder	$MgAl_2O_4$ type phase - good crystallinity
K_2O-$7Fe_2O_3$, TiO_2 doped	NBS	Received as solid, powder prepared	β-Al_2O_3 + β"-Al_2O_3 type phase + unknown phase - medium crystallinity
K_2O-$7Fe_2O_3$, TiO_2 doped VH4-2	NBS	Received as solid, powder prepared	β-Al_2O_3 type phase + unknown - medium crystallinity
K_2O-$7Fe_2O_3$, TiO_2 doped VH4-3	NBS	Received as solid, powder prepared	β-Al_2O_3 type phase + unknown - medium crystallinity

$YCrO_3$ + 5% $CaZrO_3$ #1	Trans-Tech	Powder	$YCrO_3$ type phase - medium crystallinity
$YFeO_3$ + 5% $CaZrO_3$ #1	Trans-Tech	Powder	$YFeO_3$ type phase - medium crystallinity
$Y_{.95}Mg_{.05}CrO_3$ #4	Trans-Tech	Powder	$YCrO_3$ type phase - medium crystallinity
$82HfO_2$-$18CeO_2$ #T1	ANL	Received as solid, powder prepared	∿90% monoclinic HfO_2 + ∿10% cubic (fluorite) type phase - poor to medium crystallinity
$9MgAl_2O_4$-Fe_3O_4 #2	Trans-Tech	1395°C, powder	$MgAl_2O_4$ type phase - very good crystallinity
$82HfO_2$-$18CeO_2$ #T1a	ANL	1300°C, received as solid, powder prepared	∿90% monoclinic HfO_2 + ∿10% cubic (fluorite) type phase - poor to medium crystallinity
$82HfO_2$-$18CeO_2$ #T1b	ANL	1400°C, received as solid, powder prepared	∿90% monoclinic HfO_2 + ∿10% cubic (fluorite) type phase - poor to medium crystallinity
$82HfO_2$-$18CeO_2$ #T1c	ANL	1500°C, received as solid, powder prepared	∿90% monoclinic HfO_2 + ∿10% cubic (fluorite) type phase - poor to medium crystallinity
$82HfO_2$-$18CeO_2$ #T1d	ANL	1600°C, received as solid, powder prepared	∿90% monoclinic HfO_2 + ∿10% cubic (fluorite) type phase - poor crystallinity
$4NiAl_2O_4$-Fe_3O_4	Trans-Tech	Powder	$MgAl_2O_4$ type phase - very good crystallinity
$64FeAl_2O_4$-$36Fe_3O_4$	Trans-Tech	Powder	Fe_2O_3 + Al_2O_3 - poor to medium crystallinity
$3MgAl_2O_4$-Fe_3O_4	G.E.	Received as solid, powder prepared	$MgAl_2O_4$ type phase - very good crystallinity
$82HfO_2$-$18CeO_2$ #T1a	ANL	Received as solid, powder prepared	∿90% monoclinic HfO_2 + ∿10% cubic (fluorite) type phase - poor to medium crystallinity
$82HfO_2$-$18CeO_2$ #T1b	ANL	Received as solid, powder prepared	∿90% monoclinic HfO_2 + ∿10% cubic (fluorite) type phase - poor to medium crystallinity
$74HfO_2$-$16.3CeO_2$-$9.7Y_2O_3$ #T3a	ANL	Received as solid, powder prepared	Cubic HfO_2 type phase - medium crystallinity
$74HfO_2$-$16.3CeO_2$-$9.7Y_2O_3$ #T3b	ANL	Received as solid, powder prepared	∿70% cubic HfO_2 + ∿30% monoclinic HfO_2 - poor crystallinity
$74HfO_2$-$16.3CeO_2$-$9.7Y_2O_3$ #T2	ANL	Received as solid, powder prepared	∿90% cubic HfO_2 + ∿30% monoclinic HfO_2 - medium to good crystallinity

$85ZrO_2$-$12CeO_2$-$3Y_2O_3$ CZ-CE0101a	Westinghouse	Received as solid, powder prepared	Cubic ZrO_2 - poor crystallinity
$85ZrO_2$-$12CeO_2$-$3Y_2O_3$ CZ-CE0101b	Westinghouse	Received as solid, powder prepared	Cubic ZrO_2 - very poor crystallinity
$La_{.95}Mg_{.05}Cr_{.68}Al_{.32}O_3$	Univ. Mo.	Received as solid, powder prepared	Rhombohedral perovskite type phase - medium to good crystallinity
$La_{.95}Mg_{.05}Cr_{.85}Al_{.15}O_3$	Univ. Mo.	Received as solid, powder prepared	Rhombohedral perovskite type phase - good crystallinity
$La_{.95}Mg_{.05}Cr_{.50}Al_{.50}O_3$	Univ. Mo.	Received as solid, powder prepared	Rhombohedral perovskite type phase - medium crystallinity
$La_{.95}Mg_{.05}Cr_{.50}Al_{.50}O_3$	Westinghouse	Received as solid, powder prepared	Rhombohedral perovskite type phase - medium crystallinity
$La_{.95}Mg_{.05}Cr_{.68}Al_{.32}O_3$	Westinghouse	Received as solid, powder prepared	Rhombohedral perovskite type phase - good crystallinity

2. Electrode Design and Testing

a. Phase III-U-02 (W. R. Hosler)

It is necessary to obtain the best possible arc plasma sprayed materials for the Phase III electrode module. A program was worked out with APS Materials, Inc., Dayton, OH for determining the optimum spray parameters in order to obtain the highest density, single phase materials. While there are many variables to consider, those given systematic study in the program were (1) type of torch used, (2) arc gas flow, velocity and constituent, (3) arc current, and (4) torch to substrate distance. A report on the experimental details has been received from APS Materials and is available for anyone interested. The samples resulting from the optimization program have been analyzed and are reported on elsewhere in the report.

The first of several Phase III proof tests will be carried out at the Westinghouse Research and Development Center, Pittsburgh, PA sometime during the week of October 3, 1977. A representative from NBS will be present at each test. Samples from the tests will be returned for post-test analysis. Pre-test samples from the various electrode suppliers have been received. The XRD and electrical conductivity of these materials are reported elsewhere in this report.

b. AVCO Slagging Test "A"

The anode and cathode sections for this test were delivered to AVCO Everett Research Center on August 10, 1977. The purpose of the experiment is to test several electrode configurations consisting of several materials designed in such a way as to withstand the conditions of a slagging MHD generator under load. The material just under the slag must be compatible with slag at about 1200 °C where the slag is solid, tightly bonded to the material and yet has a good electrical conductivity.

The lay-out of the electrodes and the identification system is shown in Fig. 1. Schematic diagrams of the electrodes showing the materials, thicknesses, bond line design temperatures, and material thermal conductivities are shown in Figs. 2 through 6.

All pre-test data on the materials will be given in the final report. This set of electrodes was tested for 10 hours at AVCO on September 14, 1977. Post-test analysis and materials characterization is in progress and will be reported at a later date.

c. MIT Test 185-186

Six electrodes (3 anodes and 3 cathodes) were fabricated by APS Materials, Inc., Dayton, OH according to NBS design and specifications. They were mounted on the standard MIT test rig base. A schematic design is shown in Fig. 7. Option 2 was used. The top electrode in each stack used the HfO_2-$5Y_2O_3$ cap. The other electrode used the ZrO_2-$5Y_2O_3$ cap. This test was completed May 26, with representatives from Westinghouse, APS Materials, and NBS present. The samples were returned to NBS for analysis. This analysis is completed and reported elsewhere in this report. It appears likely from the initial observations on this and previous tests that large mechanical stresses are placed on the electrode ceramics (especially the cathode) because of the thermal expansion and large temperature gradient transverse to the surface.

Another set of electrodes has been constructed but with the electrodes segmented at 20 mm intervals along the surface in an effort to relieve these stresses. These electrodes are composed of $LaCrO_3$ with a $85ZrO_2$-$3Y_2O_3$-12 CeO_2 cap. The $LaCrO_3$ is bonded to nickel on plated copper through a cermet grade using METCO 447 powder. The test will be completed in early October.

AVCO/NBS SLAGGING ELECTRODE

flow ↓

	ANODE	CATHODE
APS slag on MAFF-31 attached to Brunsbond pad Slag 1.1 mm MAFF-31 1.5 Pad 1.0	1101	2101
	1102	2102
	1103	2103
APS Slag on MAFF-31 attached to Cermet (MAFF-31 40% Cr) Slag 1.1 mm MAFF-31 1.5 Cermet 1.0	1204	2204
	1205	2205
APS MAFF-31 on Brunsbond pad MAFF-31 2.5 mm Pad 1.0	1306	2306
	1307	2307
APS MAFF-31 attached to Cermet (MAFF-31 40% Cr) MAFF-31 2.5 mm Cermet 2.5	1408	2408
	1409	2409
APS Slag on $LaCrO_3$ Slag 1.1 mm $LaCrO_3$ 2.6	1510	2510
	1511	2511

FIGURE 1.

Fig. 2. SCHEMATIC ELECTRODE DESIGN USING APS SLAG MAFF-31 AND MESH ATTACHMENT

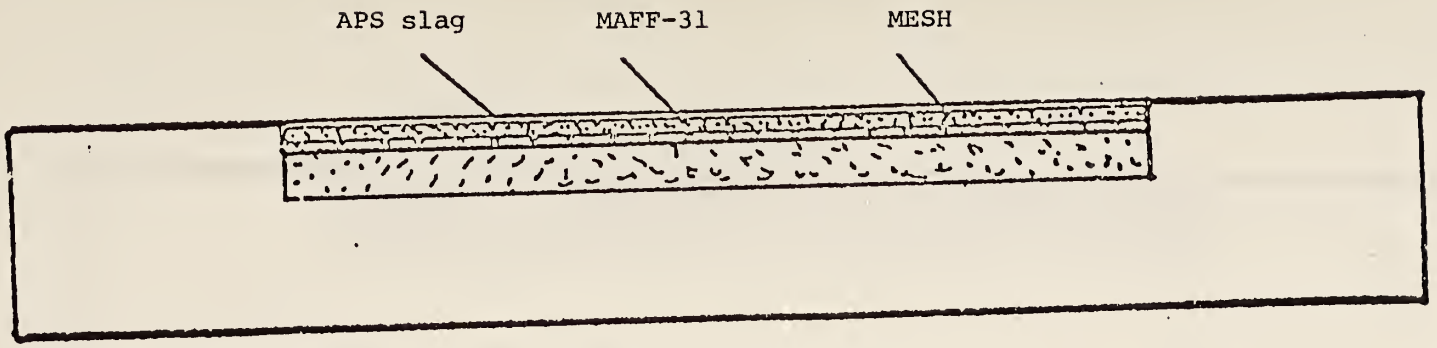

	Thickness (mm)	λ (watts/cm °C)
Mesh	1.0	.016
MAFF-31	1.5	.024
Slag	1.1	.024
Total	3.6	

Cut 3.70 mm

Make up .08 mm deficit in total thickness in MAFF-31 thickness (1.52 mm).

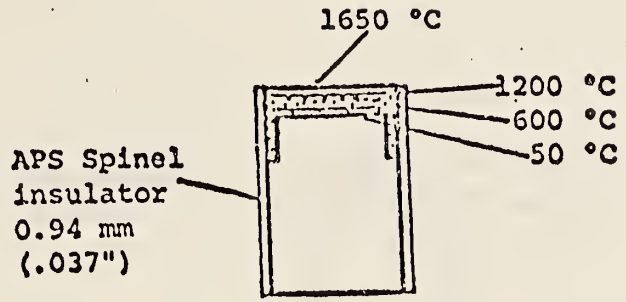

Total Width of Finished Piece 17.5 mm (0.700") $^{+0}_{-.1}$ mm

Fig. 3. SCHEMATIC ELECTRODE DESIGN USING APS SLAG, MAFF-31 AND CERMET MAFF-31 40 w/o Cr

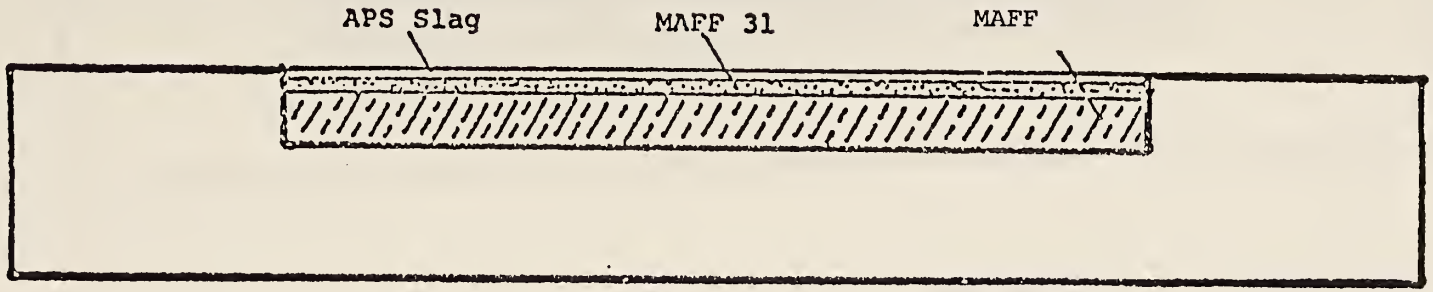

Thickness (mm)		λ (watts/cm °C)
MAFF-31-40 w/o Cr	2.5	.045
MAFF-31	1.5	.024
APS Slag	1.1	.024
Total	5.1	

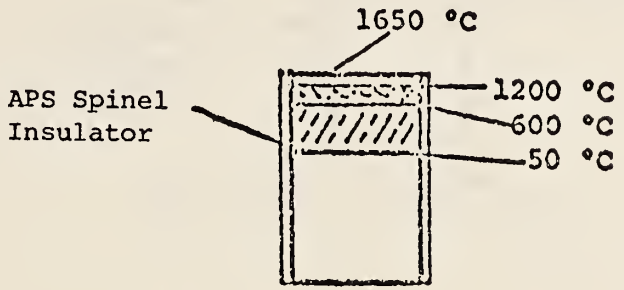

TOTAL WIDTH OF FINISHED PIECE

17.5 mm (.700") $^{+0}_{-.1}$ mm

Fig. 4. SCHEMATIC ELECTRODE DESIGN USING MAFF-31 AND MESH ATTACHMENT

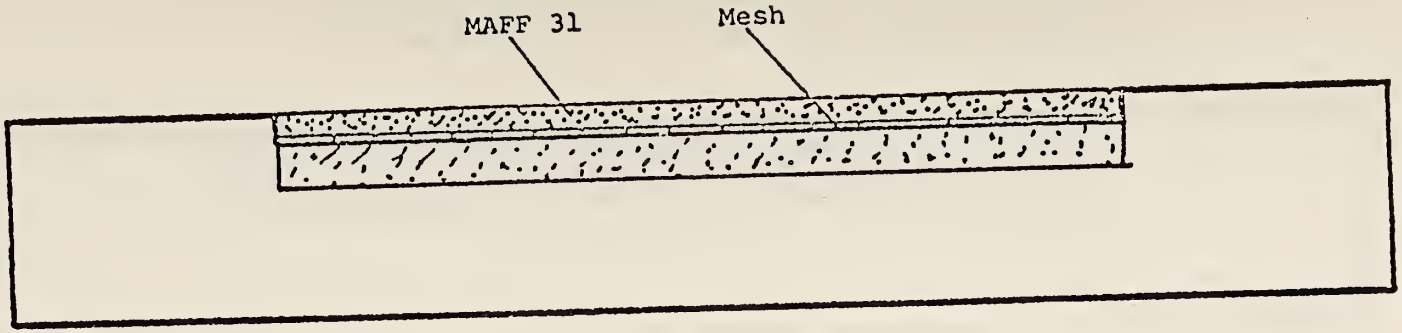

Thickness (mm)		λ (watts/cm^2)
Mesh	1.1	.016
MAFF-31	2.52	.024
Total	3.62	

Cut 3.70 mm

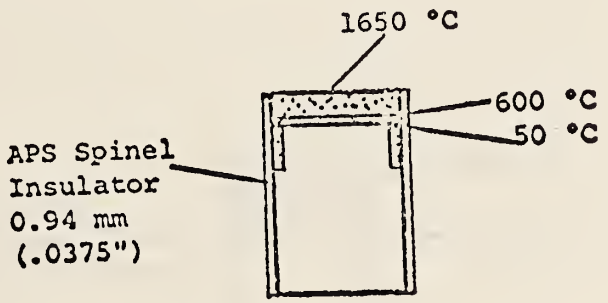

Total Width of Finished Piece 17.5 mm (0.700") $^{+0}_{-.1}$ mm

Fig. 5. SCHEMATIC ELECTRODE DESIGN USING MAFF-31 AND CERMET MAFF-31-40 w/o Cr

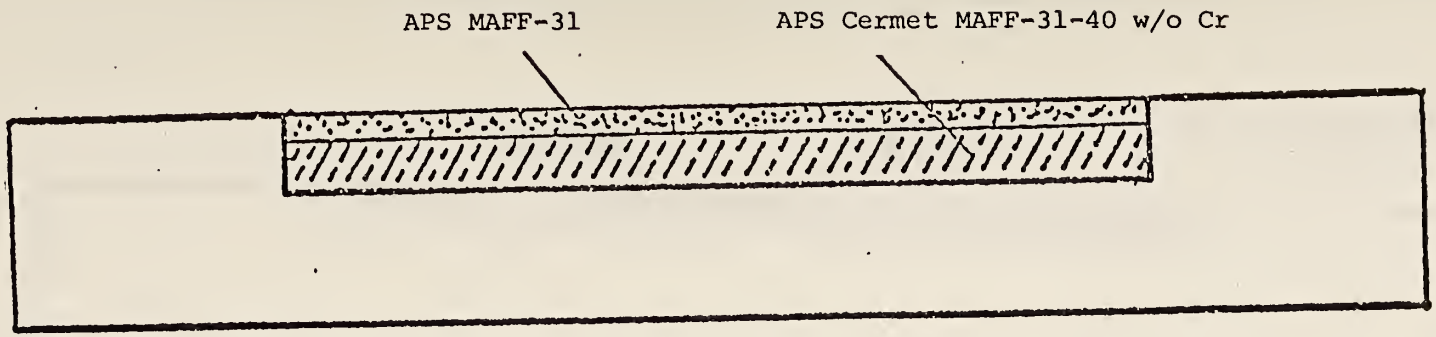

	Thickness (mm)	λ (watts/cm °C)
Cermet	2.5	.045
MAFF-31	2.5	.024
TOTAL	5.0	

Cut 5.1 mm

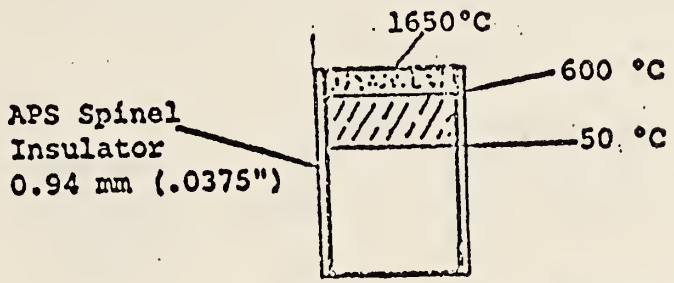

Total Width of Finished Piece 17.5mm (0.700") $^{+0}_{-.1}$ mm

Fig. 6. SCHEMATIC ELECTRODE DESIGN USING APS SLAG ON CERMET ATTACHED $LaCrO_3$ TO COPPER

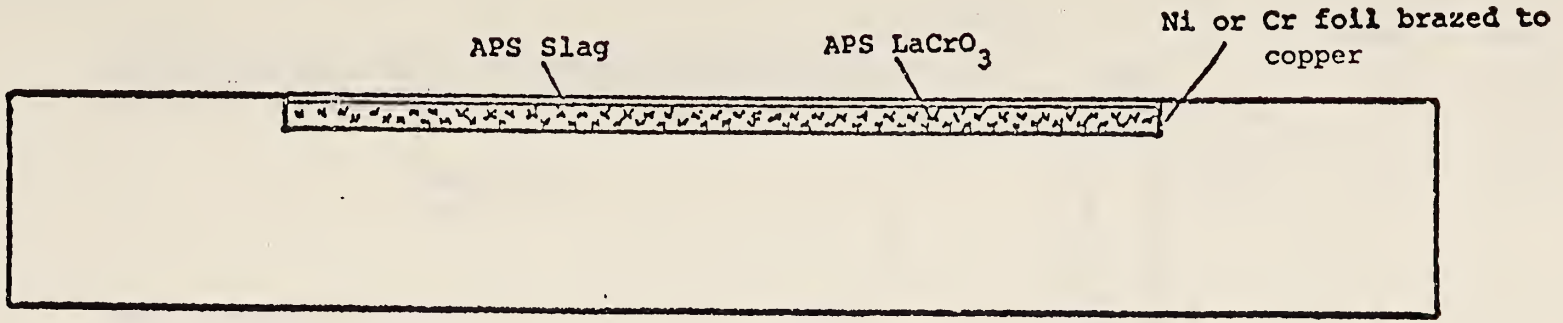

Thickness	(mm)	λ
$LaCrO_3$	2.6	.022
Slag	1.1	.024
Total	3.7	

Cut to 3.7 mm

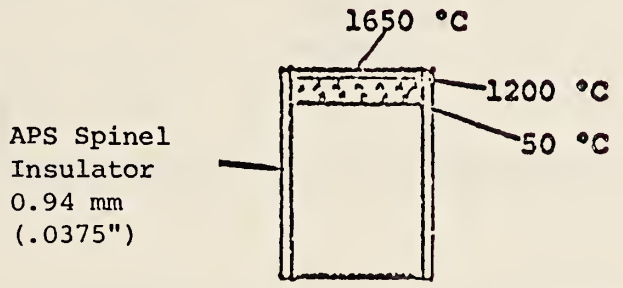

TOTAL WIDTH OF FINISHED PIECE 17.5 mm (0.700") $^{+0}_{-.1}$ mm

Figure 7. Schematic Design of MIT Test 185-186.

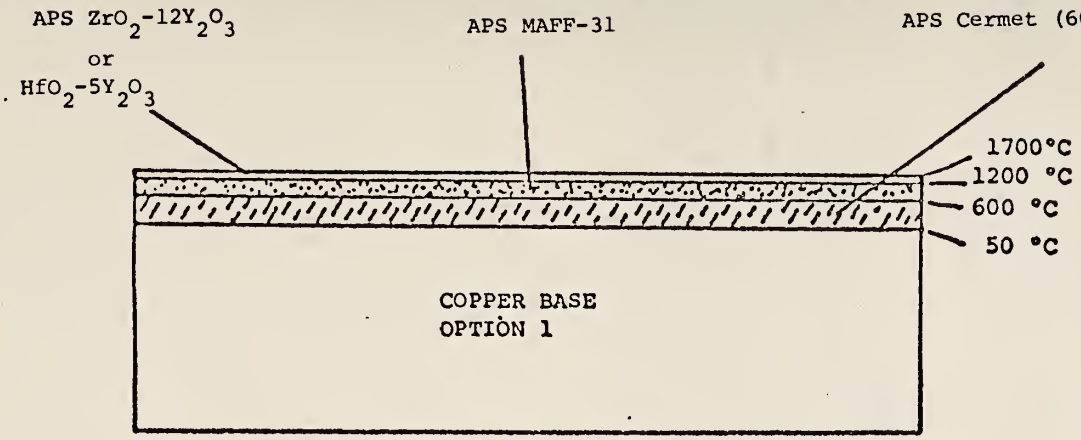

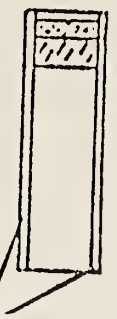

	Thickness (mm)	(watts) cm °C
ZrO_2-12Y_2O_3	0.7	0.013
MAFF-31	1.5	0.024
Cermet	2.5	0.045

APS S-71 Spinel, 0.9 mm thick, ground flat and sides parallel

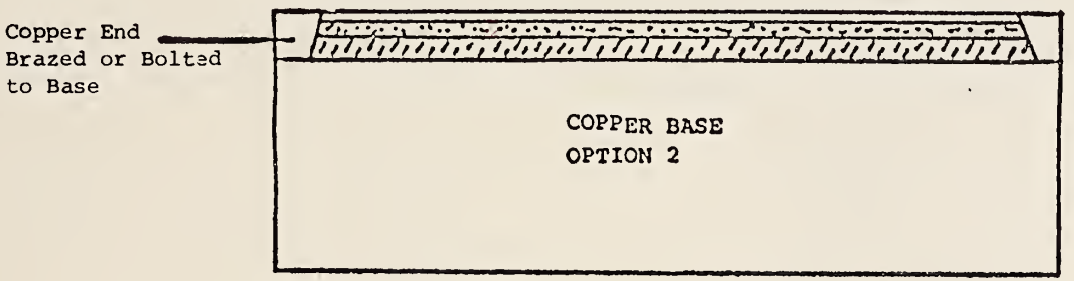

Notes:

1. Cermet joint to copper to be effected by brazing metal or alloy foil to base before APS cermet is applied.
2. All ceramic joints to be graded for maximum attachment.
3. Top of each finished electrode should be ground flat and perpendicular to the sides.

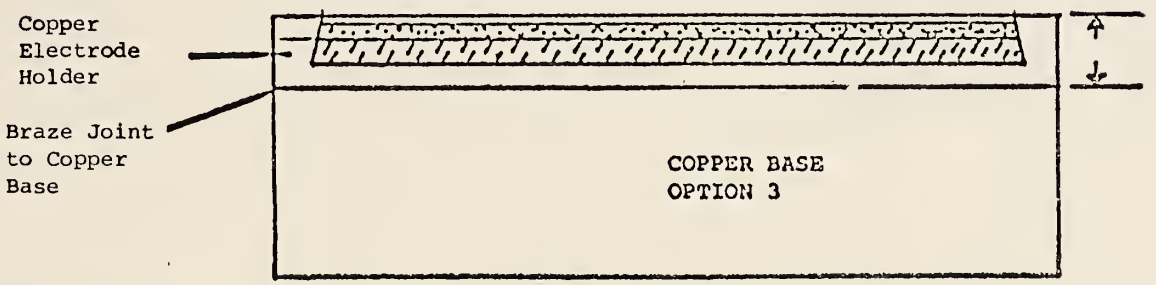

Mechanical Attachment (W. J. McKean, S. J. Schneider and W. R. Hosler)

In most concepts of a commercial generating plant involving MHD, it is conceded that repairs to the electrode walls will have to be made at certain times either on an emergency or routine basis. In order to accomplish this, it would seem advantageous to have an electrode system that could be easily removed and replaced without disassembling the channel. We have designed and built a "snap-on" electrode segment that might be used on a channel frame section. This electrode segment can be removed by mechanical force applied perpendicular to and away from the base. Conversely, it is attached or "snapped on" the base simply by applying force perpendicular to the base. This electrode piece is made of copper and is held to the channel frame element by bullet latches appropriately spaced. The ball end of the latch contacts the electrode in such a way as to place constant pressure downward to assure intimate contact between the copper electrode and the channel frame. In addition, the two copper surfaces are tinned with a solder that can be melted at the temperature of boiling water. This is done to assure good thermal and electrical contact. Electrode removal, of course, can only be done by heating the electrode above the melting point of the solder. Figures 8 , 9, and 10 show drawings of the design.

This concept is in the preliminary stage of development but an electrode using this "snap-on" configuration will be tested soon at Westinghouse Research and Development Center. It should be noted that any material ceramic or appropriate metal can be attached to the electrode copper on the plasma side. For test rigs and small experimental generators this could allow greater flexibility and increased frequency in testing. If the preliminary test at Westinghouse appears encouraging, further testing of the concept will be carried out in other test rigs using various electrode materials attached to the copper "snap on".

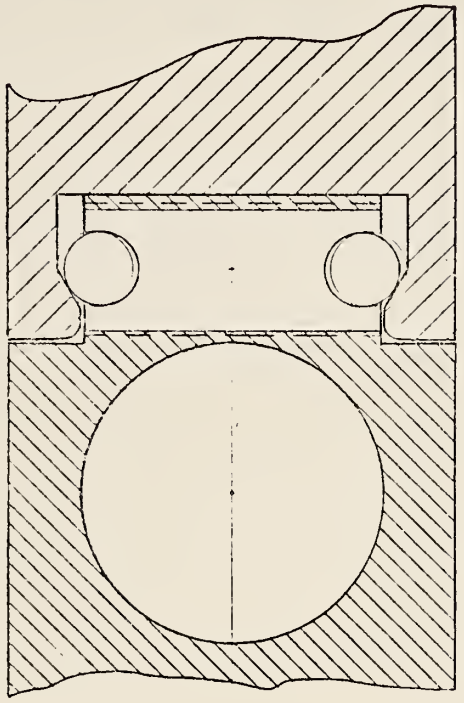

Figure 8.

ORIGINAL DATE OF DRAWING 6-9-77			
REVISIONS			
NO	E C N	CHANGE	DATE
1			
2			
3			
4			

PIECE NO	NOMENCLATURE	NO REQ'D

NATIONAL BUREAU OF STANDARDS
WASHINGTON 25 D C

ELECTRODE & HOLDER

FOR MHD

MODEL	TYPE	SCALE 10-1
DIMENSIONS IN INCHES (Unless otherwise specified)	DRAFTSMAN 1-10	CHECKED
TOLERANCES (Unless otherwise specified)	PROJECT ENGR	PROJECT ENGR
DECIMALS ± 005 FRACTIONS ± 018 ANGLES ± 4°	SUBMITTED BY CHIEF SEC	
DO NOT SCALE THIS PRINT	EXAMINED BY CHIEF ENGINEER	
DIV. SEC. 313 07 / THIS PRINT ISSUED	APPROVED BY CHIEF DIV	
	313 0020 B	

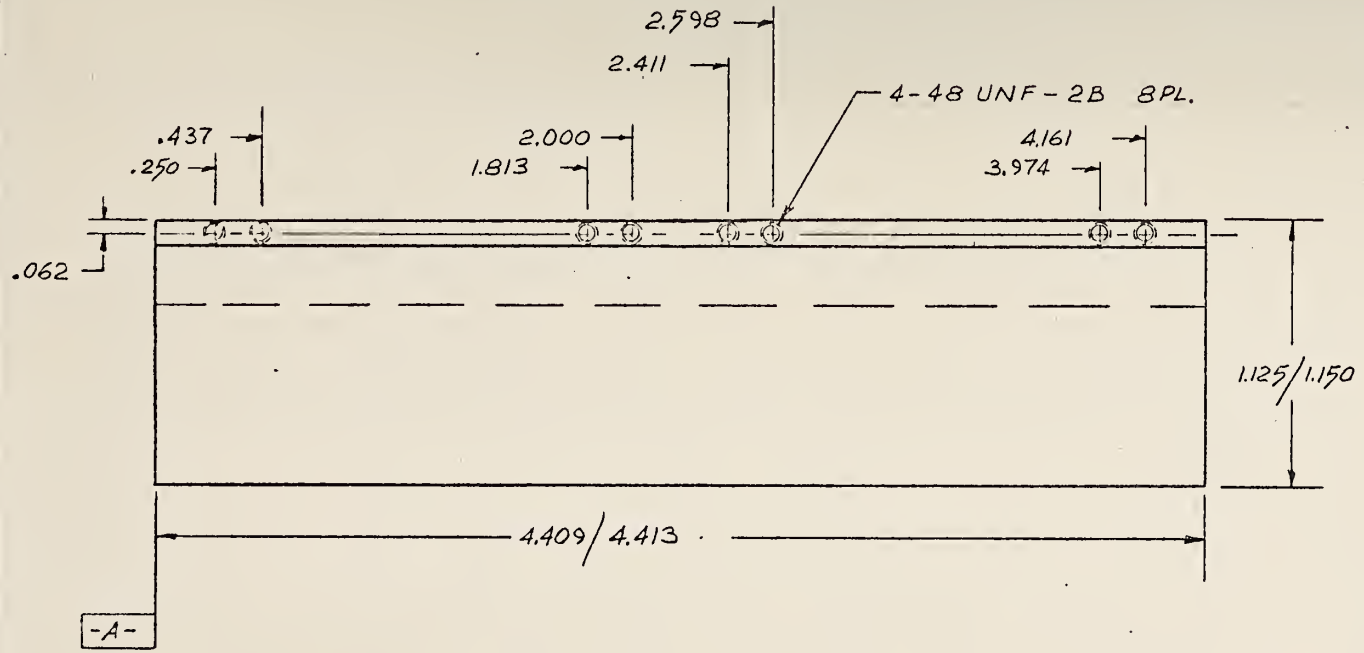

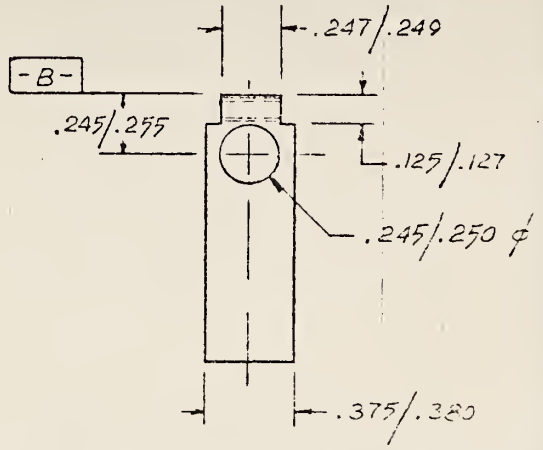

REVISIONS			
NO.	B Y N	CHANGE	DATE
1			
2			
3			
4			

MAT. HC OFC
MAKE ONE
FINISH NONE

PIECE NO	NOMENCLATURE	NO REQ'D
	HOLDER	

NATIONAL BUREAU OF STANDARDS
WASHINGTON 25, D. C.

FOR MHD

MODEL	TYPE	SCALE 2-1
DIMENSIONS IN INCHES (Unless otherwise specified)	DRAFTSMAN MD	CHECKED
TOLERANCES (Unless otherwise specified)	PROJECT ENGR	PROJECT ENGR
DECIMALS ± .005 FRACTIONS ± 1/16 ANGLES ±½°	SUBMITTED BY	CHIEF SEC.
DO NOT SCALE THIS PRINT	EXAMINED BY	CHIEF ENGINEER
DIV. SEC. 313 07	THIS PRINT ISSUED	APPROVED BY CHIEF DIV.
		313 0018 3

Figure 9.

U.S. GOVERNMENT PRINTING OFFICE: 1959 O-501997

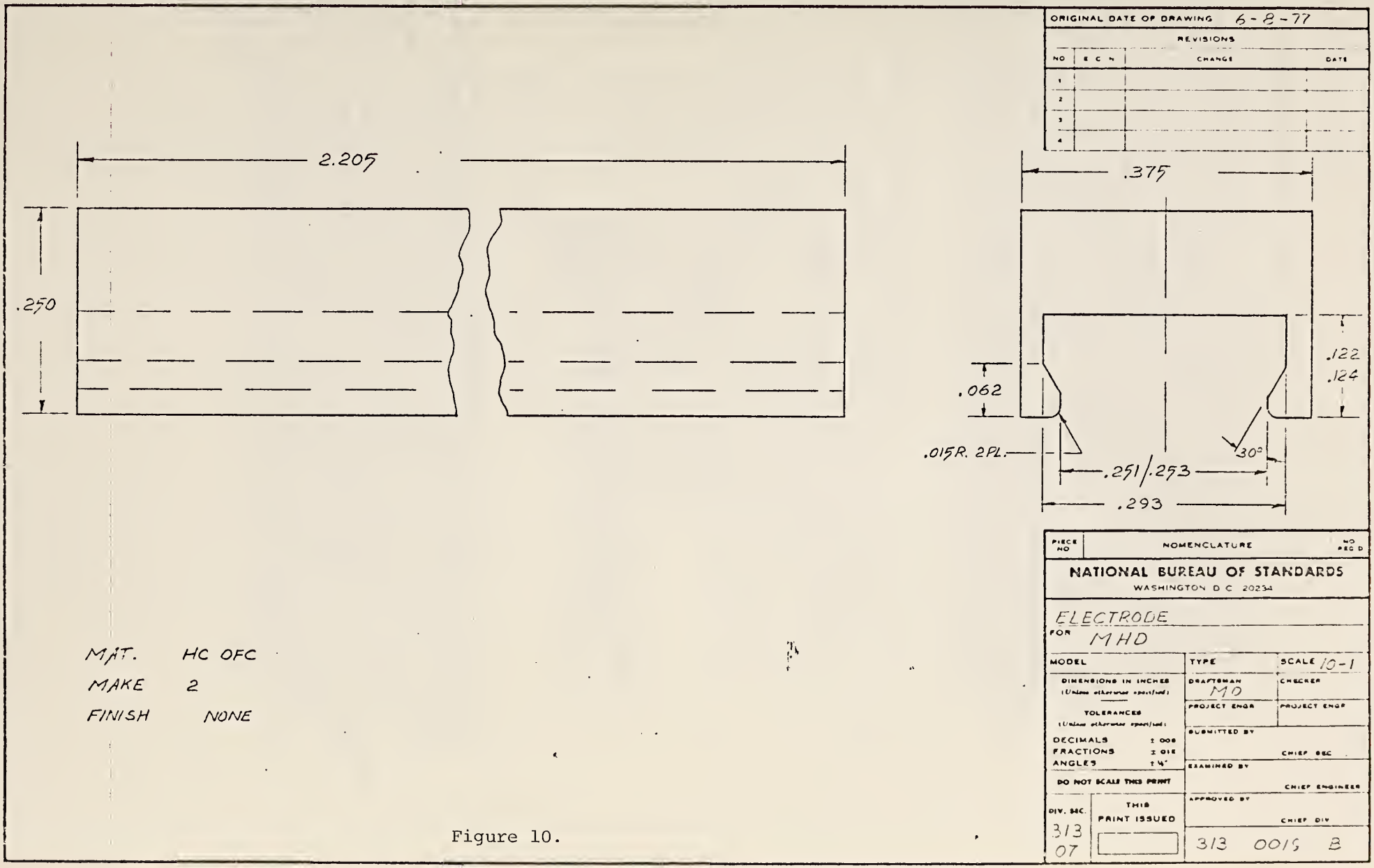
ORIGINAL DATE OF DRAWING 6-8-77
REVISIONS
NO
E C N
CHANGE
DATE
2.205
.250
.375
.062
.122
.124
.015R. 2PL.
30°
.251/.253
.293
MAT. HC OFC
MAKE 2
FINISH NONE
PIECE NO
NOMENCLATURE
NO REQ'D
NATIONAL BUREAU OF STANDARDS
WASHINGTON D C 20234
ELECTRODE
FOR MHD
MODEL
TYPE
SCALE 10-1
DIMENSIONS IN INCHES
DRAFTSMAN MO
CHECKER
TOLERANCES
PROJECT ENGR
PROJECT ENGR
DECIMALS ± 008
FRACTIONS ± 016
ANGLES ± 4°
SUBMITTED BY
CHIEF SEC
DO NOT SCALE THIS PRINT
EXAMINED BY
CHIEF ENGINEER
DIV. SEC. 313 07
THIS PRINT ISSUED
APPROVED BY
CHIEF DIV
313 0015 B

Figure 10.

3. Characterization

a. Electrodes Tested at MIT (T. Negas, W. R. Hosler)

On May 25-26, 1977, a set of NBS electrodes were tested at MIT. Figure 11 illustrates the general layout of electrodes including representative cross sections of anode and cathode (potted in epoxy) after testing. Electrodes were fabricated by APS Materials Dayton, OH according to NBS design and specifications. They were mounted on the standard MIT test rig base but were 3/8" wide to conform to the proposed U-25 window frame width. A cermet (40% Cr - 60% MAFF-31) was sprayed on the Cu blocks after these were "tinned" with a high melting Sn-based solder. The cermet is graded to pure MAFF-31 which, in turn, is graded to a "capping" material, either $88ZrO_2$-$12Y_2O_3$ or $95HfO_2$-$5Y_2O_3$. Insulation is $MgAl_2O_4$. Most materials were plasma sprayed. Electrode thicknesses were calculated using a heat flux of 100 W/cm^2 and the best available values for thermal conductivity.

The main test events were as follows,

a. 10:40 - 10:45 a.m. - cooling H_2O on and ignition,

b. 11:00 a.m. - flame out, electrodes reached ∿1400°C,

c. 11:21 - 11:43 a.m. - restart and reignition

d. 12:36 - 12:47 p.m. - temperature ∿1675°C, seed on,

e. 1:06 p.m. - HfO_2-based cap beginning to spall,

f. 1:12 p.m. - 0.5 A/cm^2 on all electrodes

g. 1:21 p.m. - slight bulging at cathode,

h. 1:30 p.m. - sudden collapse of cathode center, bulging of entire cathode, apparent melting, temperature increasing, anode in perfect shape,

i. 1:34 - 1:45 p.m. - shut-down.

As suggested by the visual observations noted above, the cathodic side sustained considerably more thermomechanical-chemical degradation. Capping materials were almost entirely absent and localized melting was apparent. The cathode cross section in Figure 11B, therefore, is not representative but includes several features visually noted during operation. The ZrO_2-based caps are detaching and appear to be "uplifting" with the detached insulators which have sintered together and have been intruded (reacted) by iron oxide. The vesicular nature of the ZrO_2-based caps also suggests partial melting while the dark discoloration is due to penetration by iron. At points where unlike materials, even when graded, are juxtaposed, the $MgAl_2O_4$ insulation is developing fractures.

It remains unclear whether detachment of "caps" results from a thermal expansion mismatch between the cap and underlying spinel or whether a combination of chemical and thermomechanical effects dominated. Significantly, the "caps" on the anodic side remained intact and fracture of the insulators is far less evident. Inspection of the "intact" interface between the cap and underlying spinel at the anode reveals one significant chemical feature. Figure 12A (50X) illustrates a typical region. The darker material (bottom) is MAFF-31 followed by a lighter material (top) via a graded zone which appears to be undergoing alteration. Hand specimens clearly reveal a thin band, reddishly discolored, for this zone. For cathodes, this band is particularly conspicuous and thick in many areas beneath the remaining caps. Fig. 12B, maps potassium (for Fig. 12A) and clearly shows that the cap-spinel interface is penetrated, and, probably, being chemically altered by condensed seed (note, this interface was designed for ∿1200°C). Fig. 13A (1000X) again shows the cap-spinel interface but clearly reveals that alteration predominates within the zone wherein ZrO_2 (Y_2O_3) and MAFF-31 previously were graded. The brighter phase is the former, the darker is the latter material. Within the upper half of Figure 13A,"islands" of unaltered ZrO_2 (Y_2O_3) are prominent (Figure 13B,map for Zr). The surrounding matrix, once spinel, now lacks cohesion, is friable and is precisely the region wherein seed is concentrated. It is tempting to conclude that the spinel portion of the graded interface is suffering from reactions with condensed seed and that this process was accelerated on the cathodic side. Development of resistive phases and poor thermal contact would accelerate excessive heating and lead to enhanced thermo-mechanical and chemical (melting) degradation.

Noted also is the highly irregular nature of the Cu/Sn-based solder/Cr-metal bond line. Figs. 14A,B (50X) shows, for example, the following sequence of materials from bottom to top, Cu/Sn-solder/ Cr-metal/cermet. Fig. 14B, far right, shows that the Cu/Sn-solder band is practically absent.

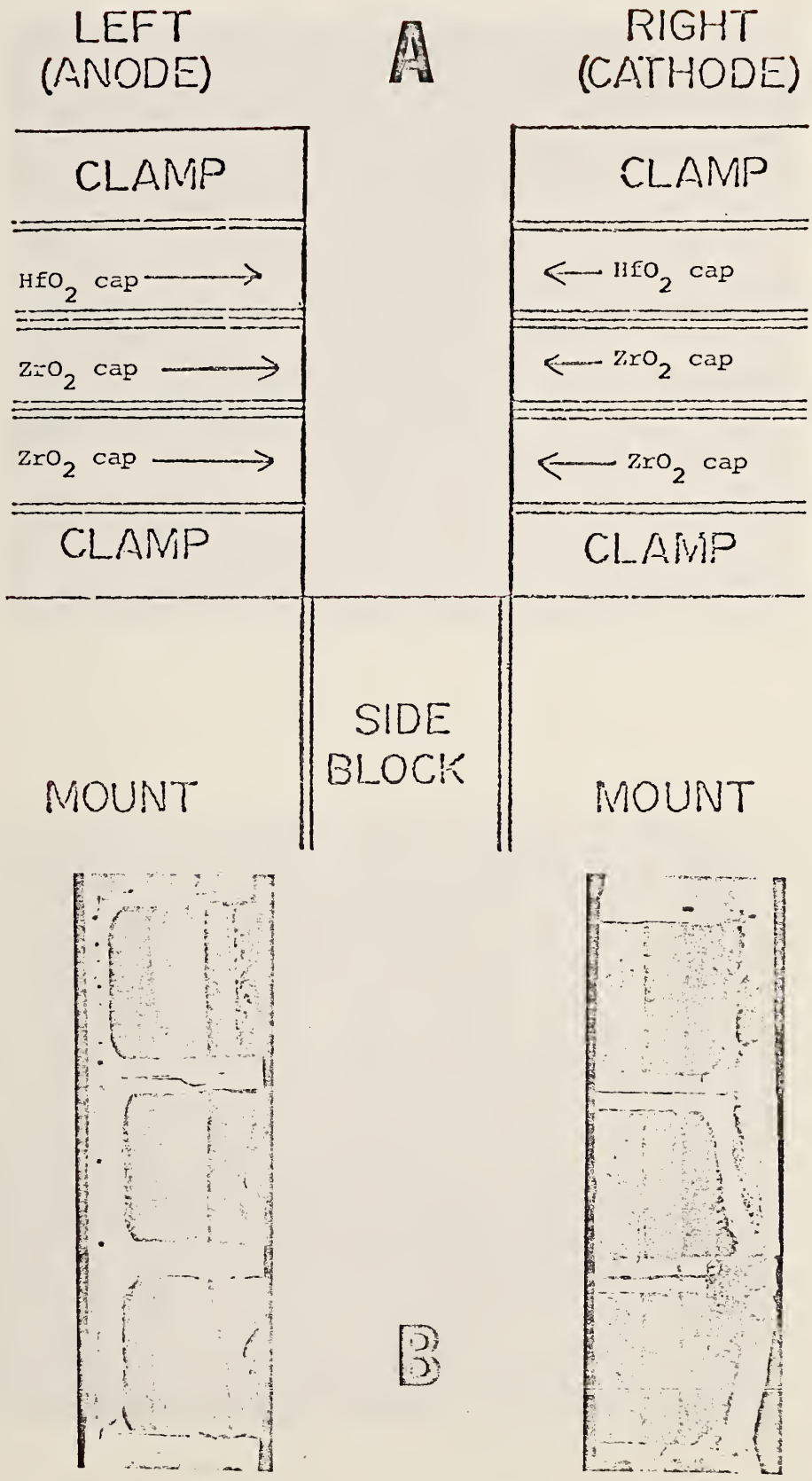

Figure 11. Surface view (A) of electrode arrangement in MIT test-rig with pertinent cross sections (B) of electrodes after testing. Plasma flow is from bottom to top.

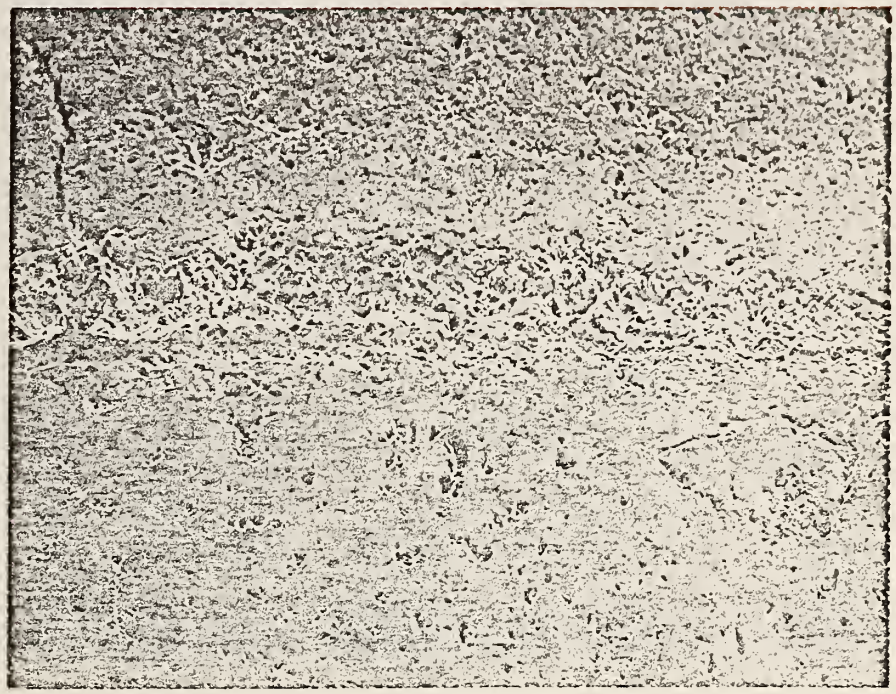

A

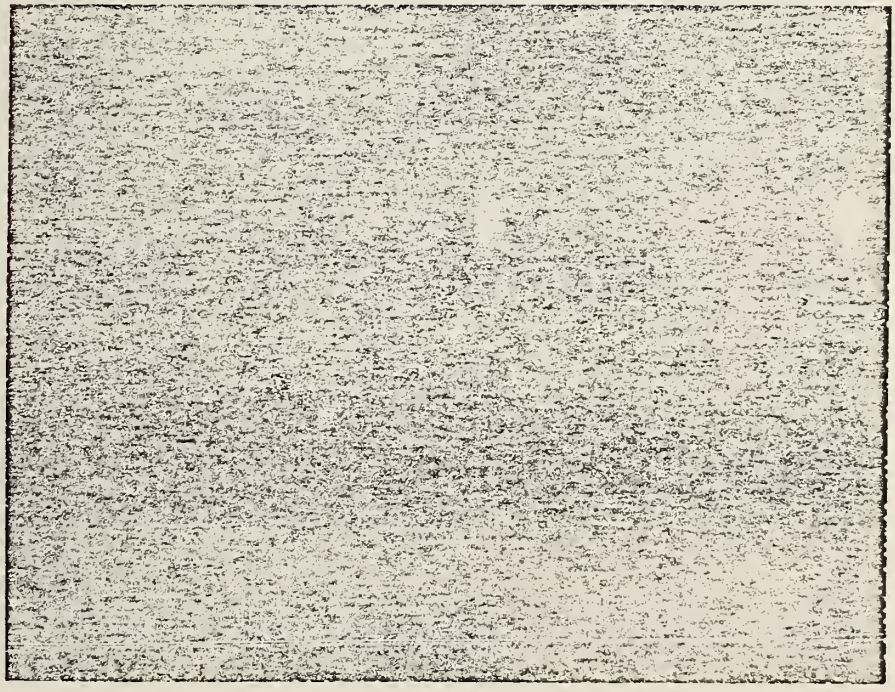

B

Figure 12. SEM micrograph (50X) in A illustrating bonding area (anode) between a ZrO_2-based cap (light material) and MAFF-31 spinel (darker material). EDX map in B shows concentration of potassium at the interface.

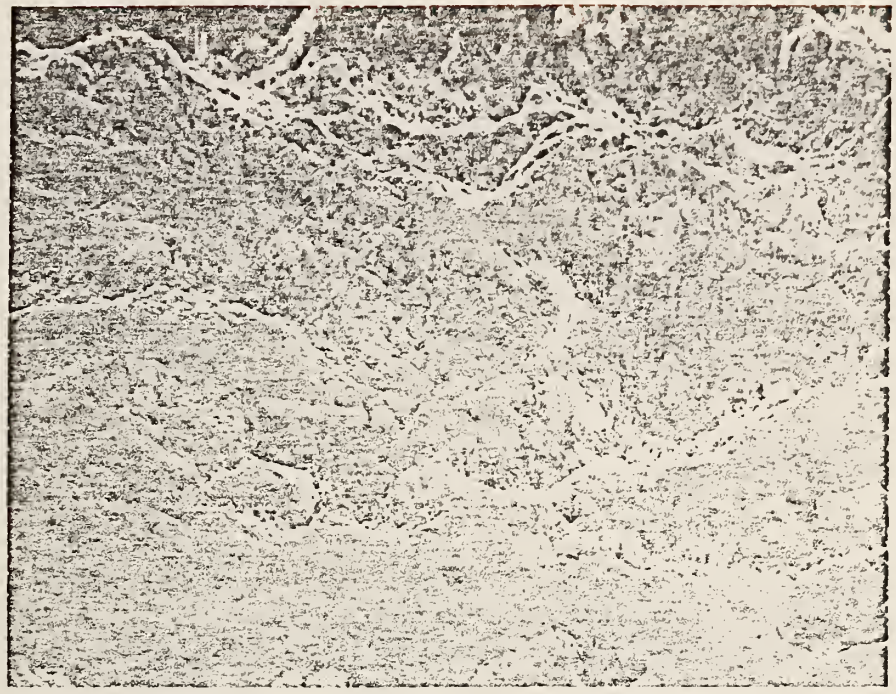

A

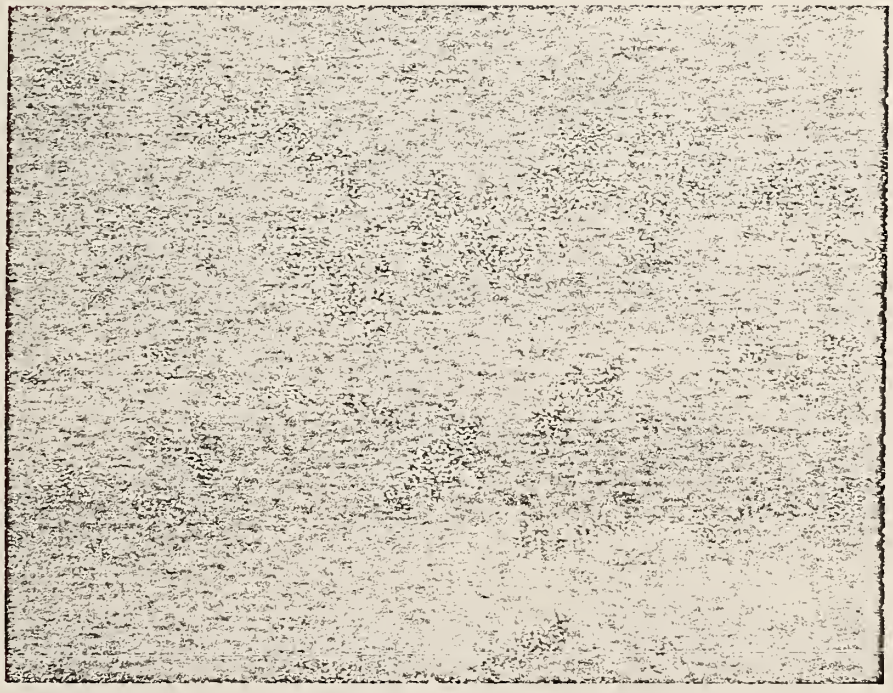

B

Figure 13. SEM micrograph (1000X) of the ZrO_2 cap-spinel interface (A) shown in Fig. 12. This region is the graded zone between spinel and the cap. EDX map in B shows distribution of Zr. See text for details.

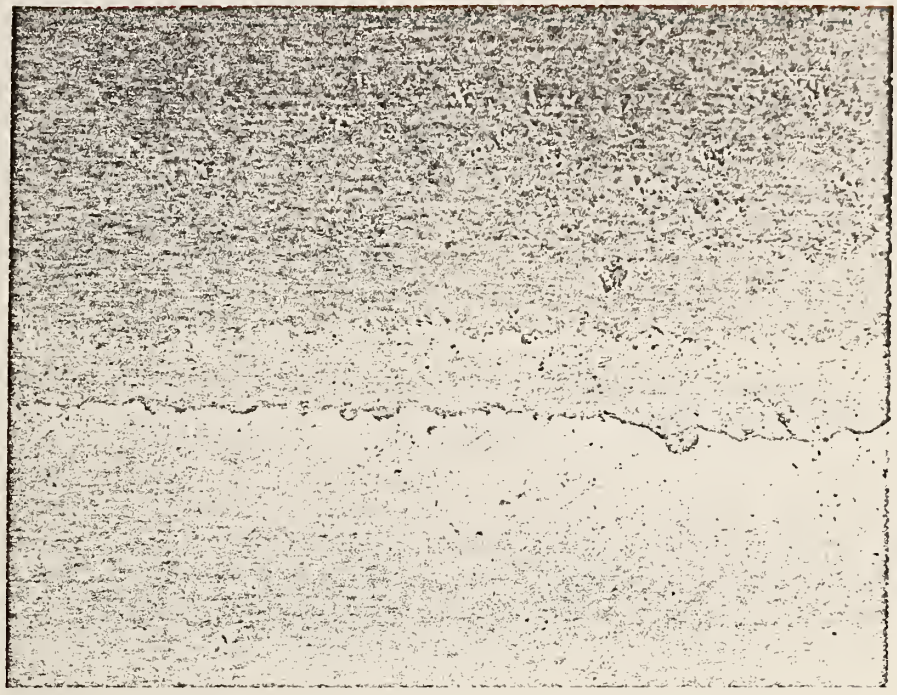

A

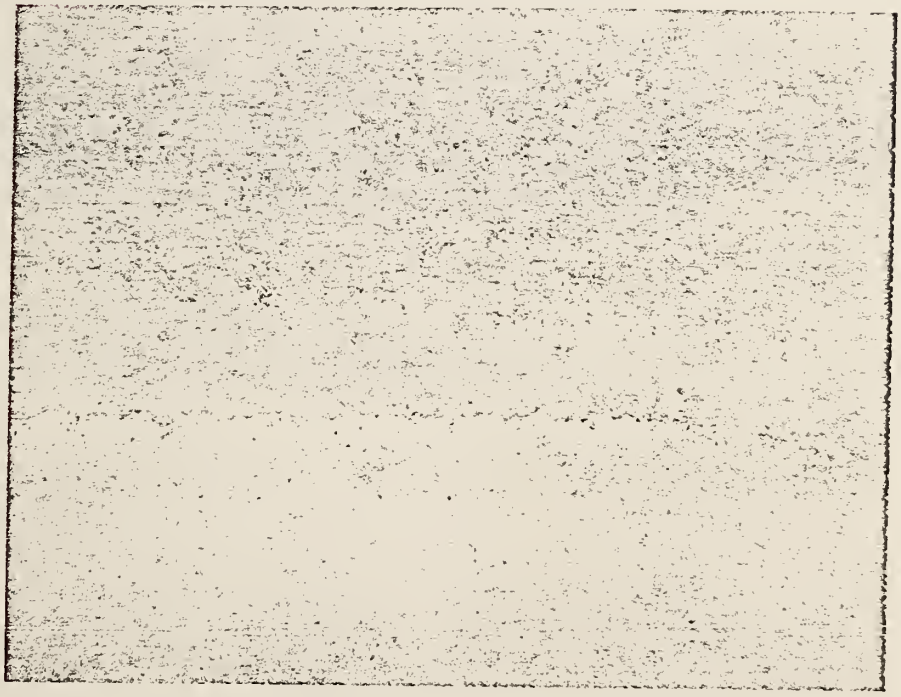

B

Figure 14. SEM micrographs (50X) illustrating discontinuous nature of bond line between Cu (lowermost material) and Sn-based solder. In A solder is continuous while in B is practically absent.

b. X-ray Examination of Fluidyne RFG Samples (A. Perloff)

Two samples of a chrome-magnesia refractory material were examined by X-ray powder diffraction techniques. The samples were FN-86 which had been cycled between 1800 - 1600 °C for 30 hours with exposure to K_2CO_3 seed (but no ash), and FN-81 which was cycled between 1800 - 1600 °C for an unspecified time period with exposure to both K_2CO_3 seed and ash. Material was chipped from the reacted layer and ground for examination. Original (untested) material, previously examined, is composed of well crystallized MgO (a = 4.212Å) and a single phase spinel (a = 8.278Å) which is probably a magnesium iron chromium aluminum oxide spinel plus traces of forsterite (Mg_2SiO_4) and monticellite-like ($CaMgSiO_4$) material.

FN-81 (K_2CO_3 and ash)

This sample is predominantly MgO (a = 4.218Å) and spinel (a = 8.260Å). The proportion of MgO relative to the spinel is clearly less than in FN-86 and the crystallinity is poorer. Some substitution of larger ions has taken place in the MgO lattice as indicated by the slight increase in the cell size. The spinel phase has also suffered more loss of the larger ions as its cell size is somewhat smaller than the previous sample. Small, but clearly identifiable, amounts of forsterite Mg_2SiO_4 and tetragonal (K-rich) $KAlSiO_4$ are present. Traces of what is probably monticellite ($CaMgSiO_4$) and hexagonal or orthorhombic $KAlSiO_4$ are also visible.

FN-86 (K_2CO_3, no ash)

This sample is predominantly MgO (a = 4.213Å) and a spinel (a = 8.268Å). The proportion of MgO relative to the spinel is approximately the same as the original material but the crystallinity is poorer (wider peaks, little $\alpha_1\alpha_2$ resolution). There is, apparently, no substitution of larger ions in the MgO lattice since there is no significant change in the unit cell dimension from that found in the original material. The spinel phase shows a slight reduction in cell size (~0.01Å) suggesting a small loss of larger Fe or Cr ions. This change is much less than found in previous samples FN-91 and FN-96 and there is not the clear splitting into two distinct spinel phases found in the earlier samples. Very small amounts of monticelitte ($CaMgSiO_4$) and K_2MgSiO_4 are visible. No visible amount of forsterite is present.

c. SEM and EDX Examination of FluiDyne Engineering Corporation tested samples.
(E. N. Farabaugh)

Four samples of a rebonded magnesia chrome spinel-iron spinel refractory (RFG) preheater material were examined. They were: FN81, cycled between 1600-1800°C in the presence of seed (K_2CO_3) and ash; FN86, cycled between 1600-1800°C for 30 hours in the presence of seed (K_2CO_3) but no ash; FN91 cycled between 1600-1800°C for 30 hours in the presence of seed (K_2SO_4) and ash; FN96, cycled between 1600-1800°C for 30 hours while exposed to ash but no seed.

The results of the examination are summarized and briefly stated as follows:

FN81

There was a rather well defined reacted layer (∿.4mm) thick which was depleted in Mg, probably at the expense of MgO. The reacted layer appeared to be a little more dense than the rest of the material. K was found to have penetrated at least 1 to 1.5 mm where it was found in material, probably $KAlSiO_4$, between the larger Cr and Fe spinel phases. Si, Ca, and Ti were also detected in amounts somewhat larger than were present in the untested material. The presence of these elements above that found in the untested material is probably traceable to some downstream source. The concentration of Mg is greatly reduced, in general, when compared to untested RFG material.

FN86

There didn't appear to be any well defined Mg depleted layer, even though the material at and near the reacted surface posses less Mg than the bulk. The drop in the concentration of Mg toward the reacted surface is much more gradual than for FN81. K has penetrated a little deeper, 3 to 4 mm, than for FN81. Again, the K was found in material surrounding the Cr and Fe phases. Si, Ca, and Ti were detected in the specimen at levels exceeding those for untested material. Si, Ca, and K were seen in intergranular material possibly forming $CaMgSiO_4$ and K_2MgSiO_4 phases. There was a densified layer (∿1mm) but there was no unique elemental distribution associated with it.

FN91

No well defined Mg depleted zone was observed, just a gradual decrease of Mg as the reacted surface was approached. The Mg, Si, K, and Ca phases were detected surrounding the spinel grains. There was a larger penetration of K, about 4 mm, in this specimen than was observed in the two previously described samples. No obvious microstructural changes were observed in going from the reacted regions to the bulk, only elemental changes in the phases of the intergranual material.

FN96

There was Mg loss observed again towards the outer edge of the specimen. However, no well defined layer could be detected. Ca and Si, coming from a downstream source was observed to have penetrated deep (∿6mm) into the specimen. The Mg, Ca, and Si phases are again present in the material surrounding the spinel grains. Once again no striking microstructural changes were seen.

In summary, all of the tested RFG material whose results are reported here, exhibit a loss of Mg (probably MgO) during testing when compared to the untested material. The loss was most pronounced in FN81 where a well defined layer Mg depleted layer could be demonstrated by mapping techniques. Possibly the action of seed and ash together accelerate the Mg depletion reaction when compared to ash-free or seed-free testing. The spinel phases in the RFG were apparently only slightly reacted, since the concentrations of Cr and Fe varied only slightly from the exposed edge to the interior (∿-6mm) of the specimen. Changes in the phases of the material constituting the intergranual material were observed in all specimens with $CaMgSiO_4$ and K_2MgSiO_4, among others probably being formed. Ca and Ti, as well as some Si were picked up by the RFG material from a downstream source.

Task L. Assessment of Steam Plant Components - (J. R. Cuthill)

This is the 9th quarterly progress report since the initiation of Task L. In the course of this Task L a number of wrought alloys have been selected for further consideration as construction materials for the steam heat exchanger tubes and similar components. This list to date of selected alloys with their pertinent mechanical properties, and with their nominal chemical compositions were given in Tables 1 and 2, respectively, under Task L in the previous Quarterly Progress Report (April 1 to June 30, 1977). Also, in the same report the ASME Boiler Code designation, maximum allowable working stresses and temperatures are given in Table 3, for those alloys that have been given code designations.

The majority of alloys included in the selected list would appear promising to varying degrees in MHD type service, on the basis of the hot corrosion results reported in the literature. Other alloys have been included because they have been considered or even specified as the construction material in key MHD studies such as the Baseline plant design and the ECAS studies but they should be carefully reconsidered in light of known performance data; or just that there are steam plant performance data and/or simulated MHD performance data on them that makes them of interest as a basis of comparison. In the 7th Quarterly report (Jan. 1 thru Mar. 30, 1977) an attempt was made to qualitatively rank the alloys in respect to their ability to resist hot corrosion attack using the data in the literature from a variety of hot corrosion tests and conditions. In the future course of this program (Task L) it is proposed to obtain experimental hot corrosion data on some of these, as well as other selected alloys. A particular effort will be made to simulate the conditions for the precipitation of a K_2SO_4 deposit on the steam heat exchange tubes. This will necessitate simulating temperatures and geometry to see if a hard deposit of K_2SO_4 builds up on the leading edge of the tube as predicted.

In this current Quarterly Report the list of "selected wrought alloys" has been reproduced in Table 1 together with references to comprehensive and readily available data compilations (Column 2) for the design engineer who needs more detailed property data then what has been included in these quarterly reports for preliminary screening purposes. It would be an unnecessarily duplication of effort to reproduce all of the readily obtainable data that may be of use in the design of a particular MHD componet. However, an attempt will be made to reproduce any difficult to obtain data that are particularly pertinent to the MHD application. One of the most comprehensive and readily available data compilations is the 5 volume Aerospace Structural Metals Handbook (1) which is published in loose-leaf form and periodically updated. The volume and Code numbers in column 2 refer to specific entries in this data compilation. Generally of equal importance with these master data compilations are the alloy producers own property data bulletins. References to these are given in Column 3. In the case of the Cr-Mo low alloy heat exchanger steels supplementary creep-rupture data have been recently compiled for the Metals Properties Council, N.Y.C. and published by ASTM (2). Also for the following steels:

(Stress Rupture Properties of:)

Mild steel
1/2% Mo steel
1% Cr 1/2% Mo steel
2 1/4% Cr 1% Mo steel
9% Cr steel
12% Cr steel
AlSl 304 stainless steel
AlSl 321 stainless steel
AlSl 347 stainless steel
AlSl 316 stainless steel

the Central Electricity Generating Board, London has included a particularly detailed set of stress-rupture curves in a recent Bulletin (3).

Salient characteristics are given in the last column of Table 1.

Table 2 is the corresponding list of nominal compositions duplicated from the previous quarterly report.

Some newly revealed experience by the power industry in the UK on the spalling of stainless steel superheater tubes on the steam side is summarized here.

Steamside Spalling of Boiler Tube Alloys

It has recently been reported (4) that in steam plants in the UK spalling of type 316 stainless steel in superheated steam at $\sim$ 565° is a normal occurance sometime after 7000 hours and has resulted in the complete blocking of tubes, overheating, and complete failure. Type 321 stainless steel, which is a titanium stabilized stainless steel, is apparently similar in behavior to type 316. However, type 347 which is a niobium stabilized stainless steel apparently oxidizes at a slower rate with smaller size flakes. The same phenonemon is observed with the ferritic stainless steels. However, apparently Incoloy 800 is much more resistant to spalling than any of the austenitic or ferritic stainless steels.

The spalling is claimed to be due to a Fe_2O_3 layer that forms on top of the Cr oxide film. It is claimed that maintaing 10 ppm or more of free hydrogen in the steam will prevent this outer layer of Fe_2O_3 from forming.

An update on the prices of many of the alloys in Table 1 has been compiled and is presented as Table 3. The prices are for material in tubular form unless otherwise marked. The prices of the Hastelloys and Haynes alloys are from the Stellite Division of the Cabot Corp. The prices of the INCO alloys are from the International Nickel Co.

In future quarterly reports, materials that have been specified for the respective components in benchmark type plant designs such as the Baseline Plant and the ECAS II designes will be listed together with the materials that this reviewer would propose.

References

1. Aerospace Structural Metals Handbook, Vols. 1 through 5, 1976 revision, Mechanical Properties Data Center, Belfour Stulen, Inc., Traverse City, Michigan.

2. Evaluation of the Elevated Temperature Fireside and Creep-Rupture Properties of 3 to 9% Cr-Mo Steels, prepared for the Metal Properties Council by G. V. Smith, ASTM Data Series Pub. DS 58 ASTM, 1916 Race Street, Philadelphia, PA 19103, (1975).

3. The Control of High Temperature Fireside Corrosion, 2nd ed., D.W.C. Baker, et.al., pub. by Central Electricity Generating Board, Sudbury House, Newgate Street, London EC1A 7AU., 20.

4. M. I. Manning and E. Metcalfe, Oxide Spalling in Stainless Steel Superheater and Reheater Tubes and Possible Control Measures, to be presented at the 6th European Congress on Corrosion, London, 19-23 Sept. 1977.

5. Handbook of Stainless Steels, 1977 edition, D. Peckner, ed., McGraw Hill, N.Y. 1977.

6. "Chromium-Nickel Stainless Steel Data", the International Nickel Company, Inc. One New York Plaza, N.Y., N.Y. 10004

7. "Allegheny Stainless Steel Technical Information", Allegheny Ludlum Steel Corporation, Pittsubrgh, PA 15222.

8. Properties Bulletins from Cabot Stellite Division, Kokomo, Ind. 46901.

9. "Huntington Alloys Handbook" and "Incoloy Alloys" of Huntington Alloy Products Division, INCO, Huntington, W. Virginia 25720.

10. "Alloy Fact Sheet", Ibid.

11. Property Bulletins from Babcock & Wilcox Company, Tubular Products Division, Beaver Falls, PA 15010.

Table 1. Selected Wrought Alloys

Stainless Steel	Compilations Property Data (References)	Producer's Property Data (References)	Salient Characteristics
1. 304	2(1302)**	(5),(6),(7)	
2. 310	2(1305)	(5),(6),(7)	Highest oxidation resistance of any stainless steel, 3 times better than 304. Low strength. Excellent resistance to H_2S (see Q.R. for 4/1-6/30/77.
3. 316	2(1308)	(5),(6),(7)	Has exhibited severe spalling in superheated steam
4. 446		(5),(7)	Highest oxidation resistance of any ferritic stainless steel
Ni&Fe-Ni base			
5. Hastelloy C-276		(8)	Superior resistance to sulfur attack. Use in desulfurization equipment
6. Hastelloy X		(8)	Resistance to stress corrosion cracking, good weldability resists oxidation to 2200 °F, high Mo may lower hot corrosion resistance
7. Haynes 556		(8)	Developmental alloy, equal to Haynes 188 in oxidation, but may be better in hot corrosion because of low W & Mo
8. Inconel 601		(9)	Resistant to sulfurdizing atmosphere. Used for radiant furnace tubes
9. Inconel 617		(10)	New alloy. Oxidation & carbonization resis. to 1100 °C.
10. Inconel 718		(9)	Oxidation resistance to 1800 °F, good weldability
11. Inconel X750		(9)	Good for springs and bellows to 1200 °F
12. Incoclad 671/800			INCO 671 can be clad to either 800 or 800 H. No strength at MHD temperature
13. Inconel 671		(9)	Best hot corrosion resistance of any alloy under MHD conditions
14. Incoloy 800H		(9)	H is for higher carbon and higher strength than Incoloy 800
15. Incoloy 800	2(1613)	(9)	Very resistant to spalling in steam heat exchanger service
16. Incoloy 802	2(1610)	(9)	Higher strength than 800, same oxidation resistance
17. Udimet U500	5(4206)	(8)	Good hot corrosion resistance, but IN-738 is better. See Q.R. for 7/1-9/30/76
o-Base Alloys			
3. Haynes 25*	5(4302)	(8)	Good formability weldability strength, oxidation resistance to 1800 °K.
9. Haynes 188	5(4310)	(8)	Better oxidation resistance than Hastelloy X. Good high temperature strength
. Croloy 9M	(2)	(11)	

ame as designation

Reference given thus, Vol. No. 2, Code No. (1302), refer to Aerospace Structural Metals Handbook, Ref. 1.

Table 2. Chemical Compositions of Selected Wrought Alloys

Item No.	Mfgr. Designation	Cr	Ni	Co	Fe	Al	Ti	Nb	Ta	Mo	W	Mn	Si	C	Other
	Stainless Steels														
1	304 S.S.	18-20	8-12	-	bal	-	-	-	-	-	-	2.0	1.0	0.08*	0.045P .03S
2	310 S.S.	24-26	19-22	-	bal	-	-	-	-	-	-	2.0	1.5	0.25*	0.045P .03S
3	316 S.S.	16-18	10-14	-	bal	-	-	-	-	2.0-3.0	-	2.0	1.0	0.08*	0.045P .03S
4	446 S.S.	23-27	0.50*	-	bal	-	-	-	-	-	-	1.5	1.0	0.35*	0.04P .025N
	Ni & Fe-Ni Base Alloys														
5	Hastelloy C-276	14.5-16.5	bal	2.5*	4-7	-	-	-	-	15-17	3-4.5	1.0*	0.05*	0.02*	0.35V .03P*
6	Hastelloy X	20.5-23.0	bal	0.5-2.5	17-20	-	-	-	-	8-10	0.2-1.0	1.0*	1.0*	1.15*	0.02La 0.2N
7	Haynes 556	22.0	20.0	20.0	bal	0.3	-	0.1	0.9	3.0	2.5	1.5	0.40	0.10	0.02La 0.2N 0.02Zr
8	Inconel 601	23.0	60.5	-	14	1.35	-	-		-	-	0.5	0.25	0.05	0.5Cu* 0.007S
9	Inconel 617	22.0	54	12.5	-	1.0	-	-		9.0	-	-	-	0.07	--
10	Inconel 718	17-21	50-55	1.0	bal	0.2-.8	0.9	(4.75-5.5)[a]		3.0	-	0.35	0.35	0.08	0.3Cu* 0.006B
11	Inconel X750	14-17	70 min.	-	5-9	0.4-1.0	2.5	(0.7-1.2)[a]		-	-	1.0	0.5*	0.08	0.5Cu 0.01S
12	Incoclad 671/800H	see below for compositions of cladding (671) and substrate (800H)													
13	Inconel 671	48	bal	-	-	--	0.35	-	-	-	-	-	-	0.05	--
14	Incoloy 800H	21	32.5	-	46	0.38	0.38	-	-	-	-	0.75	0.50	0.1	0.38Cu -.008S
15	Incoloy 800	21	32.5	-	46	0.38	0.38	-	-	-	-	0.75	0.50	0.05	0.38Cu -.008S
16	Incoloy 802	21	32.5	-	46	-	--	-	-	-	-	0.80	0.40	0.35	0.4 Cu
17	Udimet U500	15-20	bal	13-20	4.0*	2.5-3.2	2.5-3.2	-	-	3.0-5.0	-	-	--	0.15	0.008B
	Cobalt Base Alloys														
18	Haynes HS25	19-21	9-11	bal	3.0*	--	--	--	--	--	14-16	1-2	1.0*	0.10	--
19	Haynes 188	20-24	20-24	bal	3.0*	--	--	--	--	--	13-16	1.25	0.2-0.5	.05-.15	0.05-.15La
	Low-Alloy High Strength Steels														
20	Croloy 9M	8-10	--	--	--	--	--	--	--	0.9-1.1	-	0.3-0.6	.25-1.0	0.15*	0.03P 0.03S
21	HCM 9M (Japan)	8-10	--	--	--	--	--	--	--	1.8-22	-	0.3-0.7	.50*	0.08*	0.03P 0.03S

* = max

a() = Nb + Ti

* = max

Table 3. Prices of Candidate Alloys for Steam Heat Exchanger Tubes, etc. (in lots over 5000 ft.)

Alloy	2" O.D. Tubing Price/ft.	Price/lb.
Incoclad 671/800H	$28.30[a]	$11.13
Inconel 617	30.25[a]	11.50
Incoloy 802	18.50[a]	7.28
Incoloy 800	9.15[a]	3.60
Hastelloy C-276	27.22[b]	8.98
Hastelloy X	19.49[b]	6.96
Haynes 25	37.43[b]	12.00
Haynes 188	35.28[b]	11.35

[a]Price/ft. of 2" O.D. x 0.125" wall. Update of prices given in Quarterly Report for period ending June 30, 1977.

[b]Price/ft. of 2" O.D. x 0.134" wall. Prices from Stellite Division, Cabot Corp., Kokomo, Ind.